bioRxiv preprint doi: https://doi.org/10.1101/821389; this version posted October 28, 2019. The copyright holder for this preprint (which was not certified by peer review) is the author/funder, who has granted bioRxiv a license to display the preprint in perpetuity. It is made available under aCC-BY 4.0 International license.

Screening of Tau Protein Kinase Inhibitors in a Tauopathy-relevant cell-based model of Tau Hyperphosphorylation and Oligomerization

Hamad Yadikar*[1,2,4], Isabel Torres[1], Gabrielle Aiello[1], Milin Kurup[1], Zhihui Yang[1] Fan Lin[1], Firas Kobeissy[1,3], Richard Yost[4], Kevin K. Wang* [1,5]

[1] Program for Neurotrauma, Neuroproteomics & Biomarkers Research, Departments of Emergency Medicine, Psychiatry, Neuroscience and Chemistry, University of Florida, Gainesville, FL32611, USA

[2]Department of Biological Sciences, Faculty of Science, Kuwait University, P.O. Box 5969, Safat 13060, Kuwait.

[3]Faculty of Medicine, American University of Beirut Medical Center, Beirut, Lebanon.

[4]Department of Chemistry, Chemistry Laboratory Building, University of Florida, Gainesville, FL 32611, USA.

[5]Brain Rehabilitation research Center, Malcom Randall VA Medical Center, 1601 SW Archer Rd. Gainesville, FL 32608, USA.

*Correspondence:

Kevin Wang, kwang@ufl.edu ; phone: +1 (352) 328-7663

Hamad Yadikar, hamad.yadikar@ku.edu.kw; Phone: 352-900-9687

bioRxiv preprint doi: https://doi.org/10.1101/821389; this version posted October 28, 2019. The copyright holder for this preprint (which was not certified by peer review) is the author/funder, who has granted bioRxiv a license to display the preprint in perpetuity. It is made available under aCC-BY 4.0 International license.

ABSTRACT

Tauopathies are a class of neurodegenerative disorders characterized by abnormal deposition of post-translationally modified tau protein in the human brain. Tauopathies are associated with Alzheimer's disease (AD), chronic traumatic encephalopathy (CTE), and other diseases. Hyperphosphorylation increases tau tendency to aggregate and forms neurofibrillary tangles (NFT), a pathological hallmark of AD. In this study, okadaic acid (OA, 100 nM), a protein phosphatase 1/2A inhibitor, was treated for 24h in mouse neuroblastoma (N2a) and differentiated rat primary neuronal cortical cell cultures (CTX) to induce tau-hyperphosphorylation and oligomerization as a cell-based tauopathy model. Following the treatments, the effectiveness of different kinase inhibitors was assessed using the tauopathy-relevant tau antibodies through tau-immunoblotting, including the sites: pSer202/pThr205 (AT8), pThr181 (AT270), pSer202 (CP13), pSer396/pSer404 (PHF-1), and pThr231 (RZ3). OA-treated samples induced tau phosphorylation and oligomerization at all tested epitopes, forming a monomeric band (46-67 kDa) and oligomeric bands (170 kDa and 240 kDa). We found that TBB (a casein kinase II inhibitor), AR and LiCl (GSK-3 inhibitors), cyclosporin A (calcineurin inhibitor), and Saracatinib (Fyn kinase inhibitor) caused robust inhibition of OA-induced monomeric and oligomeric p-tau in both N2a and CTX culture. Additionally, a cyclin-dependent kinase 5 inhibitor (Roscovitine) and a calcium chelator (EGTA) showed conflicting results between the two neuronal cultures.This study provides a comprehensive view of potential drug candidates (TBB, CsA, AR, and Saracatinib), and their efficacy against tau hyperphosphorylation and oligomerization processes. These findings warrant further experimentation, possibly including animal models of tauopathies, which may provide a putative Neurotherapy for AD, CTE, and other forms of tauopathy-induced neurodegenerative diseases.

Keywords: Tau hyperphosphorylation, protein kinase inhibitor, okadaic acid, cell-based model, Tau oligomerization.

Background

Tauopathy is a class of neurodegenerative condition that is associated with pathological phosphorylated tau protein accumulation in the human brain. Tauopathy has been associated with

bioRxiv preprint doi: https://doi.org/10.1101/821389; this version posted October 28, 2019. The copyright holder for this preprint (which was not certified by peer review) is the author/funder, who has granted bioRxiv a license to display the preprint in perpetuity. It is made available under aCC-BY 4.0 International license.

53 several clinicopathological conditions, including chronic traumatic encephalopathy (CTE) (1),
54 traumatic brain injuries (2), post-traumatic stress disorder(3), and Alzheimer's disease (AD)(4, 5).
55 Tau is a structural protein whose function is to promote microtubule stabilization and
56 assembly, which are controlled by its phosphorylation state (6-8). In humans, the tau gene encodes
57 the tau protein and is located on chromosome 17q21 (9). The main tau protein is encoded by 11
58 exons which are subjected to alternative splicing on exon two, three, and ten forming six isoforms.
59 The six tau isoforms range from 352 to 441 amino acids. Tau isoforms vary in either having zero,
60 one, or two N-terminal inserts (exons 2 and 3) and three or four repeats region at the C-terminal
61 region (exon 10) (10, 11).

62 Tau protein consists of 79 potential phosphorylatable Serine and Threonine sites on the
63 longest isoform. At least thirty tau phosphorylation sites have been reported in healthy conditions.
64 Tau's phosphorylation state and its ability to interact with microtubule proteins are regulated by
65 various protein kinases and phosphatases (12, 13). Imbalances in the activities of tau kinases and
66 phosphatases can cause tau to become hyperphosphorylated at specific residues leading to a higher
67 tendency to dissociate from microtubules. Abnormally dissociated tau have a higher susceptibility
68 of forming larger protein aggregates, filament assembly, and bundling of pair helical filaments
69 (PHF) into neurofibrillary tangles (NFT) leading to cellular neurotoxicity(6-8, 14, 15).
70 Tau phosphorylation is carried out by a host of different kinases under physiological
71 condition. Abnormal activities of tau kinases have been associated with AD, including kinases
72 such as Src family kinase, Ca^{2+}/calmodulin-dependent protein kinase II (CaMKII); cyclin-
73 dependent kinase 5 (CDK5); casein kinase (1α/1δ/1ε/2); dual-specificity tyrosine kinase
74 phosphorylation and regulated kinase-1A/2 (DYRK1A/2), glycogen synthase-3, and Fyn
75 kinase(16, 17). Notably, a study reported that hippocampus and temporal cortex regions of the

bioRxiv preprint doi: https://doi.org/10.1101/821389; this version posted October 28, 2019. The copyright holder for this preprint (which was not certified by peer review) is the author/funder, who has granted bioRxiv a license to display the preprint in perpetuity. It is made available under aCC-BY 4.0 International license.

brain have high levels of CKII in AD when compared to controls (18). Furthermore, the tyrosine kinase Fyn has been highly researched for its implications with tau and neurodegeneration in the post-synapse N-methyl-D-aspartate receptors (NMDAR)(16, 19-21). Fyn phosphorylates tau in the N-terminal domain in neurons and plays a fundamental role in the amyloid signal transduction(16).

Several approaches for the treatment of tauopathic conditions have been investigated, including targeting tau kinases(22), activation of tau phosphatases(23), enhancing microtubule stabilization(24), tau immunotherapy(25), tau clearance(2), tau aggregation inhibition (26). Since *in vivo* tau-hyperphosphorylation results from multiple kinase activities, a single effective strategy to reverse tauopathies is still an open question. The inhibition of tau kinases using pharmaceutical drugs can lead to decreased levels of the hyperphosphorylated tau protein, thereby less aggregated tau (27-32). Several tau kinase inhibitors are in clinical trials for the treatment of tauopathies-related diseases (33). The most progressive protein kinase inhibition approach in the clinic thus far has been targeted at GSK-3β protein (30, 34).

It has been shown in AD and various other tauopathies that, tau is abnormally phosphorylated at Ser202, Ser396/404, Thr181, Thr205, and Thr231 (35, 36). The phosphorylation profile of tau residues at Ser202/Thr205 has been well-characterized in AD cases based on using specific antibodies (37). Analyzing these phosphorylation sites helps to show a pattern of relationships between tau protein phosphorylation and pathology.

Okadaic acid (OA), a protein phosphatase 1 and 2A (PP1/PP2A) inhibitor, induces tau hyperphosphorylation at pathological sites in both animal and cell-based models (38-40). OA inhibition of tau phosphatases allows the activation of multiple tau kinases, leading to its

bioRxiv preprint doi: https://doi.org/10.1101/821389; this version posted October 28, 2019. The copyright holder for this preprint (which was not certified by peer review) is the author/funder, who has granted bioRxiv a license to display the preprint in perpetuity. It is made available under aCC-BY 4.0 International license.

hyperphosphorylation (41, 42). Moreover, it has been shown that OA treatment in wild-type mice causes tauopathy-related abnormality in different regions of the brain (43).

In this study, mouse neuroblastoma culture (N2a) and rat primary cerebrocortical neuronal (CTX) culture was treated with OA, to induce tau hyperphosphorylation and oligomerization mimicking a tauopathy-relevant condition. In these experiments, we used the OA-induced tauopathy culture model to screen for different tau kinase inhibitors using immunoblotting and phospho-specific tau antibodies. Thus, it was hypothesized that using OA-induced tau hyperphosphorylation and aggregation as a tauopathy model to screen for kinase inhibitors would translate into putative neurotherapeutic targets for tauopathies-related disorders. Data from this work has shown that OA-induced tau hyperphosphorylation and oligomerization were inhibited by the different treatments. This side-by-side overview both highlights targets not well described, as well corroborates with data from targets previously studied, to be assessed in different relevant tauopathy-related *in vivo* models.

Methods

Phosphorylation Inhibitors

Ethylene glycol-bis(β-aminoethyl ether)-N,N,N',N'-tetraacetic acid (**EGTA**) (Sigma-Aldrich, St-Louis, MO, USA)**,** Dithiothreitol (**DTT**) (Sigma-Aldrich)**,** Lithium chloride (**LiCl**) (Sigma-Aldrich), N-(4-methoxybenzyl)-N'-(5-nitro-1,3-thiazol-2-yl)urea (**AR-A014418**) (Sigma-Aldrich), (9S,10R,12R)-2,3,9,10,11,12-Hexahydro-10-hydroxy-9-methyl-1-oxo-9,12-epoxy-1H-diindolo[1,2,3-fg:3',2',1'-kl]pyrrolo[3,4-i][1,6]benzodiazocine-10-carboxylic acid methyl ester (**K252a**) (Sigma-Aldrich), (2R)-2-1-butanol (**Roscovitine**) (Sigma-Aldrich), 4,5,6,7-Tetrabromo-2-azabenzimidazole (**TBB**) (Sigma-Aldrich), 1-(7-methoxyquinolin-4-yl)-3-(6-

bioRxiv preprint doi: https://doi.org/10.1101/821389; this version posted October 28, 2019. The copyright holder for this preprint (which was not certified by peer review) is the author/funder, who has granted bioRxiv a license to display the preprint in perpetuity. It is made available under aCC-BY 4.0 International license.

(trifluoromethyl)pyridin-2-yl)urea (**A-1070722**) (Sigma-Aldrich), cyclosporine A (Sigma-Aldrich), N-(5-chloro-1,3-benzodioxol-4-yl)-7-[2-(4-methylpiperazin-1-yl)ethoxy]-5-(tetrahydro-2H-pyran-4-yloxy)quinazolin-4-amine (**Saracatinib**) (Selleck Chemicals, Houston TX), (5S,6R,7R,9R)-6-methoxy-5-methyl-7-(methylamino)-6,7,8,9,15,16-hexahydro-17-oxa-4b,9a,15-triaza-5,9-methanodibenzo[b,h]cyclonona[jkl]cyclopenta[e]-as-indacen-14(5h)-one (**STS**) (ab120056; Abcam, Cambridge, MA, USA), Z-Asp-2,6-Dichlorobenzoyloxymethyl Ketone (**Z-DCB**) (Cayman Chemical, Ann Arbor Michigan) and okadaic acid (Cell Signaling Technology, Danvers, MA). SNJ-1945 was a gift from (Senju Pharmaceutical Co. Ltd., Kobe, Japan) **(Table 1)**.

Antibodies

The antibodies that were used in this study were: phospho-tau monoclonal antibodies PHF-1 (pSer396/pSer404, 1/1000), CP13 (pSer202, 1/1000), RZ3 (pThr231, 1/1000), AT8 (pSer202/pThr205, 1/1000) , AT270 (pThr181, 1/1000) and total tau monoclonal antibodies: DA9 (a.a. 102-140, 1/1000), DA31 (aa150-190, 1/1000) (gift from Peter Davies, Albert Einstein College of Medicine, Bronx, NY), polyclonal total tau DAKO (aa243-441, 1/5000) (CiteAb, England). Mouse anti-αII-spectrin (ENZO Life Sciences, Farmingdale, NY, USA, 1/5000). β-actin was used as protein loading evenness control (abcam, Cambridge, MA, USA, 1/3000) **(Table 2)**.

Cell lines and media

Brain mouse neuroblastoma N2a cells were purchased from American Type Culture Collection (ATCC #CRL-2266, Manassas, VA, USA) and were grown as recommended by the manufacturer. The cells were grown at 1:1 Dulbecco's modified Eagle medium: reduced serum Eagle's minimum essential media (DMEM: Opti-MEM) supplemented with 5% FBS (Thermo-Fisher), 100 units/mL

bioRxiv preprint doi: https://doi.org/10.1101/821389; this version posted October 28, 2019. The copyright holder for this preprint (which was not certified by peer review) is the author/funder, who has granted bioRxiv a license to display the preprint in perpetuity. It is made available under aCC-BY 4.0 International license.

144 penicillin and 0.1 mg/mL streptomycin. Cells were incubated at 37°C in a humidified 5% CO_2-
145 containing atmosphere.

146 **Primary Cerebrocortical neuronal cultures**

147 Rat primary cerebrocortical neuronal culture (CTX; Thermofisher; Cat. No. A10840) harvested
148 from a homogenized pool of day ten Sprague–Dawley rat brains and plated on poly-L-lysine-
149 coated (0.01% (w/v)) 12-well culture plates (Erie Scientific, Portsmouth, NH, USA), similar to
150 previously described methods[102] at a density of 4.36×10^5 cells/ml. Cultures were grown in
151 Neurobasal® media (Thermo Fisher), supplemented with 1% B-27 (Thermo Fisher), one mM
152 Glutamine (Thermo Fisher) and incubated at 37° C in a humidified 5% CO_2-containing
153 atmosphere. The medium was replaced every three days.

154 **Cell treatments**

155 For N2a cell culture treatments, complete media was replaced with serum-free DMEM media. For
156 CTX primary cultures, all experiments were performed after ten days in culture, and the media
157 was replaced with Neurobasal® media supplemented with 0.5% B-27. For both CTX and N2a
158 culture, SNJ-1945 (S, 100 μM) and Z-DCB (Z, 60 μM) were added to all experimental conditions
159 before the treatment for 1h. This was followed by treatment with okadaic acid (OA; 100 nM) for
160 24h followed by protein kinase inhibitors for 6h. The protein kinase inhibitors used included:
161 K252a (10 μM), AR-A014418 (60 μM), A-1070722 (60 μM), Saracatinib (100 μM), LiCl (5 mM)
162 TBB (30 μM), EGTA (five mM)**,** Roscovitine (60 μM), STS (0.5 μM), CsA (60 μM) (if added)
163 (**Table 1**).

164 **Cell Lysate Collection and Preparation**

165 The culture lysate harvesting for N2a cells and CTX culture were identical. After the treatment,
166 conditioned media were collected from each well and added into separate tubes on ice and

bioRxiv preprint doi: https://doi.org/10.1101/821389; this version posted October 28, 2019. The copyright holder for this preprint (which was not certified by peer review) is the author/funder, who has granted bioRxiv a license to display the preprint in perpetuity. It is made available under aCC-BY 4.0 International license.

centrifuged at 10,000 x g for 10 min at 4°C. Lysis buffer was added to the attached cells on the 12-well plates (100 µl per well). The Triton-X lysis buffer included: 1mM DTT, 1% phosphatase inhibitors (Sigma), 1% Mini-Complete protease inhibitor cocktail tablet (Roche Biochemicals), and 1% Triton X-100. The attached cells were then scraped down into the lysis buffer and collected into separate 1.5 ml Eppendorf tubes. The insoluble pellets from the conditioned culture media were combined with the lysed cells in the lysis buffer. The cell lysates were incubated for 90 minutes at 4°C and then centrifuged at 15,000 rpm for 15 minutes to remove cell debris.

SDS–PAGE and Western blotting

Protein concentrations of cell lysates were determined by bicinchoninic acid microprotein assays (Pierce Inc., Rockford, IL, USA) against albumin standards. Equal protein samples (20 µg) were prepared for SDS–PAGE in 8x loading buffer containing 0.25 M Tris (pH 6.8), two mM DTT, 8% SDS, and 0.02% bromophenol blue. Each sample was subjected to SDS–PAGE electrophoresis on a 4-20% precast-gels (Bio-Rad) and then transferred on to PVDF membranes. The membranes were blocked in 5% milk for 1h and then incubated with primary antibodies (1/1000) overnight. The secondary antibodies (Amersham Biosciences, UK, 1/10,000) anti-rabbit or anti-mouse IgG conjugated with alkaline phosphatase (Amersham, Piscataway, NJ, USA), were then added for 1h at room temperature. The blots were then washed with TBST, and immunoreactive bands were visualized by developing with biotin, avidin-conjugated alkaline phosphatase, nitro blue tetrazolium, and 5-bromo-4-chloro- 3-indolyl phosphate (BCIT/NBT) developer (KPL, Gaithersburg, MD, USA). A 250 kDa to 14 kDa rainbow molecular weight marker (RPN800E, GE Healthcare, Bio-Sciences, Pittsburgh, PA, USA) was loaded in the first well of the electrophoretic gel to estimate the molecular weight of each band. Quantitative evaluation of protein levels was performed via computer-assisted densitometric scanning (NIH ImageJ, version 1.6 software).

bioRxiv preprint doi: https://doi.org/10.1101/821389; this version posted October 28, 2019. The copyright holder for this preprint (which was not certified by peer review) is the author/funder, who has granted bioRxiv a license to display the preprint in perpetuity. It is made available under aCC-BY 4.0 International license.

Statistical Analysis

Statistical analysis was performed with one-way ANOVA Tukey's Test. For multiple comparisons, one-way ANOVA followed by the Bonferroni's post-hoc test was performed. *p<0.05, **p<0.01, ***p<0.001, **** p<0.0001, ns: non-significant. GraphPad Prism 8.0 (GraphPad, La Jolla, CA).

Results

Okadaic acid (OA), a potent PP2A/PP1 inhibitor, is known to induce tau hyperphosphorylation and aggregation (43, 44). To establish our tauopathy-relevant cell model, mouse neuroblastoma N2a cells were treated with okadaic acid (OA) (100 nM) to induce tau hyperphosphorylation and oligomerization for 6h and 24h (**Figure 1a, b**). This specific concentration of OA was selected based on other studies that used similar concentrations optimized on neuronal cell culture (38, 44-46).

Since OA is known to induce apoptosis (47), cell-permeable calpain (SNJ-1945) and caspase-3 (Z-DCB) inhibitors were included in all of our experimental conditions in order to eliminate modifications resulting from cell metabolism/health (48, 49). To assess cell viability, caspase-3, and calpain activation, the samples were probed for for αII-spectrin integrity. αII-spectrin is a key substrate for cysteine proteases associated with necrosis (calpain) and apoptotic (caspase-3) cell death (50). Cleavage of αII-spectrin by calpain produces major spectrin break down products (SBDP) of molecular weight 150 kDa (SBDP150) and 145 kDa (SBDP145), while caspase-3 activation produces major cleavage product of 120 kDa (SBDP120) detectable by Western blotting (50, 51). Our control samples probed with αII-spectrin detected only a high molecular weight 240 kDa band (intact αII-spectrin); while SBDPs were absent, suggesting a healthy metabolism and neuronal culture **(Fig1a)**. Western blots were analyzed with total tau

bioRxiv preprint doi: https://doi.org/10.1101/821389; this version posted October 28, 2019. The copyright holder for this preprint (which was not certified by peer review) is the author/funder, who has granted bioRxiv a license to display the preprint in perpetuity. It is made available under aCC-BY 4.0 International license.

monoclonal antibody DA9 (a.a. 102-140) and monoclonal phospho-tau antibodies including CP13 (pSer202) and PHF-1 (pSer396/pSer404) (**Table 1**). β-actin was probed to evaluate the evenness of loading the protein extracts. Untreated control showed that the total tau antibody DA9 detected tau protein bands at 46 kDa and 48 kDa at 6h and 24h (**Figure 1a**). The intensity of the band at 46 kDa was detected at higher levels compared to the band at 48 kDa in control samples. (**Figure 1a**).

Treatment with OA (100 nM) for 6h and 24h showed a dramatic decrease in levels of the 46 kDa and increased levels of 48 kDa with DA9 antibody. One might presume that the 46 kDa and 48 kDa bands are different tau isoforms. However, how OA treatment affected these bands suggests that they are representative of phosphorylated (p-tau) and non-phosphorylated tau (tau) rather than being tau isoforms. Thus, in our study,the 46 kDa was assigned as tau and the 48 kDa as p-tau.

Additionally, treatment with OA showed high molecular weight (HMW) band clusters residing at 170 kDa probed with DA9 antibody (a.a 102-145) for 6h ($p<0.05$) and at 24h ($p<0.0005$). These (HMW) bands may represent the formation of tau oligomers as they were not observed in control cells and only with OA-treated cells. It has been reported in a recent study that treatment with OA in human neuroblastoma SH-SY5Y cells induced tau phosphorylation and oligomerization (44). Another study showed that a local injection of OA in mice induces tau phosphorylation and aggregation in different anatomical brain regions (43). Because the tau phosphorylation and formation of HMW bands were observed relatively at higher levels with OA treatment for 24h compared to the 6h, the 24h treatment was selected as our tauopathy model (**Figure 1a, 1b**).

On the other hand, in our cell culture experimental conditions, treatment with OA (100 nM) for less than 6h did not show any detectable tau bands with CP13 and PHF-1 (data not shown).

bioRxiv preprint doi: https://doi.org/10.1101/821389; this version posted October 28, 2019. The copyright holder for this preprint (which was not certified by peer review) is the author/funder, who has granted bioRxiv a license to display the preprint in perpetuity. It is made available under aCC-BY 4.0 International license.

It is well-known that OA induces apoptosis in human neuroblastoma cells, mouse neuroblastoma, and rat cerebellum neurons (47). Thus, the time points were not increased beyond 24h of treatment to avoid tau phosphorylation modifications resulting from proteolysis and neural death.

Probing with CP13 (pSer202) antibody did not show any detectable bands of tau protein in control samples **(Figure 1a)**. This result indicates that endogenous phosphorylation of tau at Ser202 site is low under normal growth conditions. However, with OA treatment, CP13 showed HMW band formed at 110 kDa (x2 size of monomeric tau) with 6h and 24h (**Figure 1a, 1b**). Probing with PHF-1 antibody (pSer396/pSer404) did not show any tau band with control samples (**Figure 1a, 1b**). Treatment with OA for 6h and 24h showed HMW cluster of bands at 220 kDa, 240 kDa, and 260 kDa with PHF-1 (**Figure 1a, 1b**). Notably, the 260 kDa band (red arrow) (**Figure 1a**) was only detectable with OA treatment for 24h (PHF-1).

Low molecular weight monomeric tau (LMW-MT) bands were not detected with either CP13 or PHF-1. It should be noted that the DA9 antibody recognizes total tau epitopes from aa. 102-140. Thus, to identify the same 48 kDa tau species detected with DA9, the phospho-tau antibody needs to recognize the same epitope. It was assumed that LMW-MT might be either phosphorylated at sites other than Ser202/Ser396/Ser404, and LMW-MT oligomerized into the different HMW tau species detected at 110 kDa, 170 kDa, 220 kDa, 240 kDa, and 260 kDa. Indeed, using RZ3(pThr231) and AT270(pThr181), LMW-MT at 48 kDa and 55 kDa was detected with OA treatment; respectively **(Supplementary Figure 1a, left panel, OA lane)**.

Taken together, these data strongly suggest that OA treatment caused protein phosphatase inhibition inducing the formation of LMW and HMW tau bands, immunoreactive at pSer202 (CP13, 110 kDa), pSer396/pSer404 (PHF-1, 220/240/260 kDa), RZ3 (pThr231, 48 kDa) and

bioRxiv preprint doi: https://doi.org/10.1101/821389; this version posted October 28, 2019. The copyright holder for this preprint (which was not certified by peer review) is the author/funder, who has granted bioRxiv a license to display the preprint in perpetuity. It is made available under aCC-BY 4.0 International license.

AT270 (pThr181, 55 kDa). Based on the molecular weight of each species, the immunoreactivity with tau antibodies solidifies the notion of tau hyperphosphorylation and oligomerization.

Screening of tau kinase inhibitors on OA-induced tau hyperphosphorylation and oligomerization in N2a cells.

To screen for protein kinase inhibitors as drug candidates for inhibition of OA-induced hyperphosphorylation and oligomerization, mouse neuroblastoma N2a cells were pre-treated with OA for 24h followed by treatment with protein kinase inhibitors for 6h. The positive control included only OA treated cells for 24h. Protein kinase inhibitors used included: LiCl (10 mM), AR-A014418 (AR) (60 μM), A-1070722 (A107)(60 μM), K252a (10 μM), STS (0.5 μM) 4,5,6,7-tetrabromobenzotriazole (TBB) (60 μM), Roscovitine (60 μM), Saracatinib (100 μM), cyclosporine A (CsA) (60 μM), and EGTA (5 mM) (**Table 1; Figure 2a, 2b).** All conditions were pre-treated with SNJ-1945 (calpain inhibitor, abbreviated as S; 60 μM) and Z-DCB (caspase inhibitor, abbreviated as Z; 100 μM) to minimize apoptotic pathways activation (calpain and caspase-mediated proteolysis) (48, 52) (**Table 1**). To assess cell integrity, the αII-spectrin antibody was used to monitor intact-240 kDa, SBDP150, and SBDP120 that are representatives of apoptosis, necrosis, calpain, and caspase activation, respectively.

Casein kinase II (CKII) inhibitor: 4,5,6,7-tetrabromobenzotriazole (TBB)

Since aberrant CKII has been reported in AD (53), TBB, a cell-permeable CKII inhibitor, was selected for the study. Total tau DA9 showed that TBB abolished the 48 kDa band (p-tau) and the HMW 170 kDa band (tau oligomers), and significantly increased ($p<0.0001$) levels of the 46 kDa (non-phospho tau) by 85%, compared to OA treatment alone (**Figure 2a, 2b, Table 3**). CP13 (pSer202) antibody showed that TBB eliminated the OA-induced 110 kDa band (oligomeric p-

bioRxiv preprint doi: https://doi.org/10.1101/821389; this version posted October 28, 2019. The copyright holder for this preprint (which was not certified by peer review) is the author/funder, who has granted bioRxiv a license to display the preprint in perpetuity. It is made available under aCC-BY 4.0 International license.

tau). Similarly, PHF-1 antibody (pSer396/pSer404) showed that TBB fully inhibited the formation of 240 kDa (HMW bands-oligomeric tau) (**Figure 2a, 2b, Table 3**). As a selective casein kinase II (CKII) inhibitor, TBB showed robustness in inhibiting both OA-induced tau hyperphosphorylation and oligomerization. Thus, the aim was to evaluate the TBB dose-response effect on OA-induced tau hyperphosphorylation and oligomerization in N2a neuronal culture. To achieve this aim, N2a cells were treated with OA for 24h followed by treatment with various concentrations of TBB (10 nM, 30 nM, 100 nM, 300 nM, 1 µM, 3 µM, 10 µM, and 30 µM) for 6h (**Figure 3a, 3b**). The result shows that treatment with ten micromolars of TBB resulted in 50% reduction of the 110 kDa (oligomeric p-tau form; CP13), 48 kDa, and 170 kDa bands (monomeric and oligomeric p-tau, DA9) (**Figure 3a, 3b**). Increasing the concentration of TBB up to 30 µM caused 90% reduction of 48 kDa (monomeric p-tau, DA9), 170 kDa (oligomeric p-tau, DA9) and 110 kDa (oligomeric tau form, CP13) (**Figure 3a, 3b**). As for assessing neuronal culture integrity, the intact αII-spectrin band was detected at 240 kDa, and no SBDP150/145 or SBDP120 was observed with the TBB treated conditions suggesting a healthy culture.

Calcineurin Inhibitor: Cyclosporin A (CsA)

Cyclosporin A (CsA) has been reported to inhibit calcineurin phosphatase activity (PP3) and CaMKII by blocking the Ca++ mitochondrial permeability (54) (Table 1). Thus, CsA was selected in this study as a calcium-dependent kinase inhibitor to assess its effect on OA-induced tau hyperphosphorylation and oligomerization. Notably, CsA abolished the 48 kDa and 170 kDa monomeric and oligomeric p-tau of DA9, respectively (**Supplementary Figure 1a**). Moreover, CsA significantly reduced the protein band at 110 kDa of CP13 (oligomeric p-tau band; $p<0.0001$), and 240 kDa of PHF-1 (oligomeric p-tau band) (**Supplementary Figure 1a, b, Table 3**). Phosphorylation sites at human tau threonine 181 and 231 have been shown to differentiate AD

bioRxiv preprint doi: https://doi.org/10.1101/821389; this version posted October 28, 2019. The copyright holder for this preprint (which was not certified by peer review) is the author/funder, who has granted bioRxiv a license to display the preprint in perpetuity. It is made available under aCC-BY 4.0 International license.

patient from a control subject (35, 55). Hence, RZ3 (pT231) and AT270 (pT181) antibodies were used to study these sites.

RZ3 antibody showed a complete reduction of the 48 kDa band (monomeric p-tau) when cells were treated with CsA (**Supplementary Figure 1a, b**). As for AT270 antibody, OA-treated samples showed a band detected at 55 kDa (monomeric p-tau) which was abolished when neurons were treated with CsA. The 48 kDa and 55 kDa OA-induced bands detected by RZ3 and AT270, respectively, indicate that tau can have various levels of oligomerization, or can still be monomeric, depending upon the phosphorylation site tested. β-actin protein levels remained even in all experimental conditions. As for testing neuronal injury and apoptotic pathway activation, αII-spectrin blotting did not detect any significant changes of the 240 kDa band (intact form). Moreover, SBDP150/145 or SBDP120 immunoreactive bands were not detected in all of the treated samples, indicative of a healthy metabolism.

Calcium chelator: EGTA

Another calcium-dependent kinase inhibitor, EGTA, was used as a calcium-chelating agent. EGTA has a lower binding affinity for Mg^{++} relative to EDTA, making it more selective for Ca^{++} ions (56). Total tau DA9 showed that EGTA treatment (with calpain and caspase inhibitors; S+Z) caused 25% reduction of the 48 kDa band (p-tau), 85% increase of the 46 kDa band (non-phospho-tau) and 55% reduction of the 170 kDa band (oligomeric p-tau form), compared to OA treatment alone (**Figure 2a, 2b and Table 3**). Additionally, EGTA caused 90% reduction of 110 kDa band (oligomeric tau; CP13) and 85% reduction of 240 kDa (oligomeric tau; PHF-1) (**Figure 2a, 2b and Table 3**). As for apoptotic pathway activation, αII-spectrin antibody did not show any effect on the 240 kDa band (intact form), and the SBDP150/145 or SBDP120 bands were not detected with EGTA treatment.

bioRxiv preprint doi: https://doi.org/10.1101/821389; this version posted October 28, 2019. The copyright holder for this preprint (which was not certified by peer review) is the author/funder, who has granted bioRxiv a license to display the preprint in perpetuity. It is made available under aCC-BY 4.0 International license.

326 **Glycogen synthase kinase-3 (GSK-3) inhibitors: LiCl, A-1070722, and AR-1014418**

327 Tau is a substrate of Glycogen synthase kinase-3 (GSK-3)(57), and p-tau phosphorylation
328 and oligomerization could be inhibited by GSK-3 inhibition. To test this hypothesis, the effects of
329 small molecule GSK-3 inhibitors, LiCl, A-1070722 (abbreviated as A-107), and AR-1014418
330 (abbreviated as AR) were examined on OA-induced tau hyperphosphorylation and
331 oligomerization. Surprisingly, LiCl showed an opposite effect in N2a cell treatment by increasing
332 levels of 110 kDa band (oligomeric form, CP13; -14%) and levels of 240 kDa band (oligomeric p-
333 tau, PHF-1; -9%) (**Figure 2a, 2b and Table 3**). As for total tau DA9 antibody, LiCl also showed
334 an opposite effect by increasing the 48/46 kDa (p-tau/non-phospho-tau) band ratio by 20%, and
335 the 170 kDa oligomeric tau band by 12%.

336 AR, a thiazole class inhibitor, was shown to decrease insoluble p-tau in the brain stem of
337 transgenic mice overexpressing a mutant human tau protein (58). In our experimental design, AR
338 did not show a statistically significant effect on the 240 kDa band (oligomeric p-tau; PHF-1) or
339 110 kDa band (oligomeric p-tau form; CP13) (**Supplementary Figure 2a, b, Table 3**). Moreover,
340 probing with total tau DA9 showed that AR treatment caused an adverse effect by increasing the
341 48 kDa/46 kDa ratio (monomeric tau form; -50%) and reducing the 170 kDa oligomeric form band
342 by 36% (**Supplementary Figure 2a, b, Table 3**).

343 Another potent GSK-3 inhibitor, A-107 (Ki=0.6 nM for GSKα and GSK-3β) (59), was
344 selected for the study. OA followed by A-107 treatment showed 23% reduction of 110 kDa
345 oligomeric form band (CP13) and non-significant but partial reduction of the 240 kDa oligomeric
346 p-tau form (PHF-1) compared to OA treatment alone (**Supplementary Figure 2a, b, Table 3**).
347 Probing with total tau DA9 showed with A-107 treatment, a 13% reduction of 170 kDa band (DA9)
348 and did not show a statistically significant effect on the 48 kDa band (**Supplementary Figure 2a,**

bioRxiv preprint doi: https://doi.org/10.1101/821389; this version posted October 28, 2019. The copyright holder for this preprint (which was not certified by peer review) is the author/funder, who has granted bioRxiv a license to display the preprint in perpetuity. It is made available under aCC-BY 4.0 International license.

b, Table 3). As for caspase-3, calpain, and cell injury activation, αII-spectrin did not show SBDP 150/145 or SBDP120 post-treatment, indicative of a healthy neuronal culture.

Src/Fyn kinase inhibitor: Saracatinib

Saracatinib is an inhibitor of the Src/abl kinase family, developed initially for several types of cancer but withdrawn for the lack of effectiveness (60). However, Saracatinib is also a potent inhibitor of Fyn kinase, which is linked to tau (16). Fyn has been reported to phosphorylate dendritic tau, which allows Fyn to localize to the post-synaptic density (16). In the current study, Saracatinib was selected to investigate the role of Fyn kinase function on the tauopathy-relevant cell-based model. Probing with DA9 (a.a. 102-140) antibody, Saracatinib resulted in 40% reduction in the 48 kDa (monomeric p-tau), 20% increase in 46 kDa (non-phospho tau) bands and 45% reduction of the 170 kDa band (oligomeric p-tau form) (**Figure 2a, 2b, Table 3**). Saracatinib treatment caused significant reduction ($p<0.0001$) of the 110 kDa oligomeric p-tau band of CP13 (75%; CP13) and produced 46% reduction in immunoreactivity of the 240 kDa (oligomeric p-tau form band of PHF-1) (**Figure 2a, 2b, Table 3**). As for assessing cell integrity, intact spectrin (240 kDa) levels remained constant, and SBDP150/145 and SBDP120 levels were not significantly altered, with Saracatinib treatment, compared to control values.

Pan kinase inhibitor: K252a and STS

K252a is a non-selective cell-permeable protein kinase inhibitor, inhibiting protein kinase C (PKC; IC50=32.9 nM), Ca2+/calmodulin-stimulated phosphodiesterases (IC50=1.3-2.9 μM), serine/threonine protein kinases (IC50=10-20 nM), myosin light-chain kinase (MLCK; Ki=20 nM), receptor tyrosine kinases, and inhibiting the carcinogenic properties of MET oncogene (61, 62). K252a is an analog of staurosporine (STS) and has a broad spectrum of protein kinases

bioRxiv preprint doi: https://doi.org/10.1101/821389; this version posted October 28, 2019. The copyright holder for this preprint (which was not certified by peer review) is the author/funder, who has granted bioRxiv a license to display the preprint in perpetuity. It is made available under aCC-BY 4.0 International license.

inhibition, neuroprotection properties, and improvement in psoriasis in vivo (Table 1) (63). In this study, K252a and STS treatment similarly showed 30% increase in 46 kDa (monomeric non-phosphorylated tau) and 35% decrease at 48 kDa (monomeric p-tau) compared to OA, with DA9 antibody (**Figure 2a, 2b, and Table 3**). K252a treatment caused 40% reduction of 170 kDa (DA9; oligomeric p-tau) compared to OA treatment alone (average of n=3) (**Figure 2a, 2b, and Table 3**). For p-tau detection, probing with CP13 antibody showed 60% and 32% reduction in 110 kDa (oligomeric p-tau form) with K252a and STS treatment, correspondingly. PHF-1 showed 70% and 80% reduction in levels of 240 kDa (oligomeric form) with K252a and STS treatment, respectively (**Figure 2a, 2b, Table 3**). αII-spectrin immunoreactive bands (intact-240 kDa, SBDP150/145, and SBDP120) did not show a statistically significant difference compared to control values. Although STS is known to induce apoptosis, the absence of SBDPs is due to the effect of caspase and calpain inhibitors (S+Z), which in our previous studies have shown to decrease SBDP150/145/120 resulting from STS treatment (64, 65).

CDK5 inhibitor: Roscovitine

Roscovitine is a cyclin-dependent kinase 5 (CDK5) that acts through direct competition at the ATP-binding site (66). It has been previously shown that tau protein can be a hyperphosphorylated by CDK5 in specific pathological conditions (67-69). To study the role of CDK5 in our tauopathy cell-based-model, Roscovitine was selected to assess its effect on OA-induced tau hyperphosphorylation and oligomerization. Surprisingly, Roscovitine showed an adverse effect by increasing levels of oligomeric tau detected at 170 kDa (-51%; DA9), 110 kDa (-11%; CP13), and 240 kDa (-53%; PHF-1) compared to OA treatment alone (**Figure 2a, 2b, Table 3**). Roscovitine showed partial but a statistically non-significant decrease in the 48 kDa (monomeric p-tau) band of DA9, compared to OA treatment alone. Moreover, αII-spectrin antibody did not show a

bioRxiv preprint doi: https://doi.org/10.1101/821389; this version posted October 28, 2019. The copyright holder for this preprint (which was not certified by peer review) is the author/funder, who has granted bioRxiv a license to display the preprint in perpetuity. It is made available under aCC-BY 4.0 International license.

394 statistically significant difference of intact form (240 kDa), SBDP150/145, and SBDP120
395 compared to control values. β-actin protein levels remained even in all experimental conditions.

396 **Baseline and OA-induced tau hyperphosphorylation and oligomerization: effects of various**
397 **kinase inhibitors treatments in rat primary cerebrocortical neuronal (CTX) culture.**

398 To further expand our experimental paradigm in a cell-based model suitable for drug candidate
399 screening, the effectiveness of the protein kinase inhibitors was investigated on rat primary
400 cerebrocortical neuronal (CTX) cultures. Our CTX primary culture is fully differentiated neurons,
401 which can provide a model for physiologically relevant cellular events that make neurons uniquely
402 susceptible to disease-associated proteins. Additionally, the use of high-throughput primary
403 culture allowed us to screen multiple drug candidates in a short period, compared to conventional
404 methods and permit the exposure of novel biological concepts to identify new drug targets for
405 therapeutics. Therefore, CTX cells were pre-treated with or without OA 24h (100 nM) (Table 1)
406 followed by treatment with protein kinase inhibitors for 6h. Calpain and caspase-3 inhibitors, SNJ-
407 1945 and Z-DCB respectively, were added to all experimental conditions to prevent cell death-
408 mediated proteolysis of tau as a potential confound. To monitor neuronal culture health and
409 metabolism, the samples were probed with αII-spectrin antibody, and intact form (240 kDa),
410 SBDP150/145, and SBDP120 were quantified and compared to control.

411 CTX control cultures showed normal cell bodies and healthy neurites, including axons and
412 dendrites. Notably, untreated control samples showed basal levels of phosphorylated tau (67 kDa)
413 detected by total and p-tau antibodies, including: DA31 (a.a.150-190), CP13 (pSer202), RZ3
414 (pThr231), PHF-1 (pSer396/pSer404), AT8 (pSer202/pThr205), and AT270 (pThr205) (**Figure**
415 **4a, 4b, lane 1**). In agreement with previous reports using immunocytochemistry and western
416 blotting, rat cortical neurons in primary culture showed that tau is physiologically highly

bioRxiv preprint doi: https://doi.org/10.1101/821389; this version posted October 28, 2019. The copyright holder for this preprint (which was not certified by peer review) is the author/funder, who has granted bioRxiv a license to display the preprint in perpetuity. It is made available under aCC-BY 4.0 International license.

417 phosphorylated (70). Thus, in our experimental design, various kinase inhibitors were tested on
418 basal and OA-induced p-tau to measure their effects in reducing physiological and pathological
419 phosphorylation levels at different epitopes.

420 Treatment with OA for 24h caused a dramatic increase of 67 kDa band (monomeric p-tau) at
421 multiple phospho-tau epitopes (CP13: 9x, RZ3: 9.8x, PHF-1: 13x, AT8: 3x, and AT270: 10x)
422 (**Figure 5a, 5b, lane 2**). In contrast to N2a cells, oligomeric forms of tau protein were not observed
423 when tested with total tau (DA31 and DA9), and phospho-tau antibodies in CTX culture. Since
424 the samples were prepared under SDS-reducing conditions, it might be possible that tau oligomers
425 in CTX culture are disrupted, although tau cross-linking by disulfide bonds is not an essential
426 requirement for tau oligomerization (71).

427 Since the concentration of 30 μM TBB resulted in at least 90% inhibition in N2a cells, the same
428 concentration was used for CTX culture. Treating CTX culture with TBB reduced basal and OA-
429 induced tau phosphorylation (67 kDa) at CP13 (-OA: 91%, +OA: 98%), RZ3 (-OA: 100%, +OA:
430 100%), PHF-1 (-OA: 100%, +OA: 100%), AT8 (-OA: 91%, +OA: 100%), and AT270 (-OA:
431 100%, +OA: 100%) compared to OA treatment alone (**Figure 4a, 4b, lane 7 and Figure 5a, 5b,**
432 **lane 8, Table 4**). Total tau DA31 (a.a. 150-190) antibody detected immunoreactive bands at 63
433 kDa and 67 kDa with the different kinase inhibitor treatments. The decreased electrophoretic
434 mobility of the 63 kDa might correspond to the lower levels of p-tau protein induced by the protein
435 kinase inhibitors; thus, this band was assigned as non-phospho-tau. TBB treatment caused a
436 reduction of the phospho-tau band at 67 kDa (-OA: 41%, +OA: 91%), and an increase of non-
437 phospho tau band at 63 kDa (-OA: +53%, +OA: +81%) (**Figure 4a, 4b, lane 7 and Figure 5a, 5b,**
438 **lane 8, Table 4**).

bioRxiv preprint doi: https://doi.org/10.1101/821389; this version posted October 28, 2019. The copyright holder for this preprint (which was not certified by peer review) is the author/funder, who has granted bioRxiv a license to display the preprint in perpetuity. It is made available under aCC-BY 4.0 International license.

In contrast to N2a cells, LiCl caused considerable reduction of basal and OA-induced tau phosphorylation (monomeric p-tau, 67 kDa) in CTX culture at CP13 (-OA: 94%, +OA: 50%), RZ3 (-OA: 89%, +OA: 100%), PHF-1 (-OA: 98%, +OA: 100%), AT8 (-OA: 100%, +OA: 81%), AT270 (-OA: 100%, +OA: 100%) and total tau DA31 (-OA:93%, +OA:96%) (**Figure 4a, 4b, lane 4 and Figure 5a 5b, lane 5, Table 4).** AR also abolished the 67 kDa band with basal and OA-induced tau hyperphosphorylation (**Figure 4a, 4b, lane 10 and Figure 5a 5b, lane 11, Table 4**). With total tau DA31 (a.a. 150-190), LiCl and AR completely reduced the 67 kDa (monomeric p-tau) and substantially increased the 63 kDa band (non-phospho tau). Treating CTX cells with A107 also showed a substantial inhibition of 67 kDa (-OA and +OA) band with CP13 (-OA: 92%, +OA: 36%), RZ3 (-OA: 79%, +OA: 70%), PHF-1 (-OA: 65%, +OA: 85%), AT8 (-OA: 82%, +OA: 21%), AT270 (-OA: 100%, +OA: 100%), and total tau DA31 (-OA: 80%, +OA: 55%), compared to OA treatment alone (**Figure 4a, 4b, lane 9 and Figure 5a 5b, lane 10, Table 4**). As for Roscovitine treatment, in contrast to N2a neuronal treatment, the 67 kDa band was reduced considerably at CP13 (-OA: 85%, +OA: 63%), RZ3 (-OA: 42%, +OA: 91%), PHF-1 (-OA: 63%, +OA: 81%), and total tau DA31 (-OA, +OA: ~30%). However, Roscovitine did not show a statistically significant effect on OA-induced tau phosphorylation at AT8 and AT270 (**Figure 4a, 4b, lane 6 and Figure 5a 5b, lane 7, Table 4**).

On the other hand, CsA caused a molecular weight shift in the electrophoretic mobility of the 67 kDa to 63 kDa at the sites CP13 (pSer202), RZ3 (pThr231), and DA31 (a.a.102-145), presumably accounting for the dephosphorylation of tau (Supplementary Figure 3). In reference to the 67 kDa band, CsA had dramatic inhibition on basal tau phosphorylation at: CP13 (90%), RZ3 (91%), PHF-1 (89%), AT8 (95%), AT270 (92%) and total tau DA31 (67 kDa, 95%) (**Supplementary Figure 3a, b, Table 4**). With OA treatment, CsA also showed a considerable immunoreactivity reduction

bioRxiv preprint doi: https://doi.org/10.1101/821389; this version posted October 28, 2019. The copyright holder for this preprint (which was not certified by peer review) is the author/funder, who has granted bioRxiv a license to display the preprint in perpetuity. It is made available under aCC-BY 4.0 International license.

of 67 kDa band at the epitopes: CP13 (33%), AT8 (86%) and total tau DA31 (28%). CsA had no effect on 67 kDa band at PHF-1, AT270, and RZ3 compared to OA treatment alone (**Supplementary Figure 3a, b, Table 4**). Minor oligomeric bands were observed at 240 kDa with PHF-1 antibody in OA treated samples. Based on the αII-spectrin blot, CTX cultures demonstrated intact spectrin (240 kDa) and the absence of any SBDPs, suggesting a healthy metabolism under the experimental conditions.

Furthermore, Saracatinib caused considerable reduction of basal and OA-induced tau hyperphosphorylation at: CP13 (-OA: 41%, +OA: 100%), RZ3 (-OA: 81%, +OA: 100%), PHF-1 (-OA: 52%, +OA: 100%), AT270 (-OA: 0%, +OA: 84%) and total tau DA31 (-OA: 5%, +OA: 20%). Saracatinib did not show any significant effect at AT8 phospho-tau epitope (pSer202/pThr205 sites) (**Figure 4a, 4b, lane 8 and Figure 5a, 5b, lane 9; Table 4).**

Treatment with K252a caused substantial inhibition of 67 kDa band, with basal and OA-induced treatments at CP13 (-OA: 35%, +OA: 41%), RZ3 (-OA: 45%, +OA: 37%), PHF-1 (-OA: 61%, +OA: 63%), and total tau DA31 (-OA: 41%, +OA: 45%) (**Figure 4a, 4b, lane 2, and Figure 5a, 5b, lane 3; Table 4**). K252a did not show any statistically significant inhibition at AT8 and AT270 with both basal and OA-induced tau hyperphosphorylation (**Figure 4a, 4b, lane 2; 5a, 5b, lane 3; Table 4**). Cultures treated with STS showed considerable reduction of basal and OA-induced tau phosphorylation at CP13 (-OA: 86%, +OA: 63%), RZ3 (-OA: 83%, +OA: 81%), PHF-1 (-OA: 55%, +OA: 89%), AT8 (-OA: 88%, +OA: 12%), AT270 (-OA: 100%, +OA: 100%), and total tau DA31 (-OA: 41%, +OA: 45%) (**Figure 4a, 4b, lane 3a and Figure 5a, 5b, lane 4; Table 4**).

Unexpectedly, EGTA caused an adverse effect in CTX culture by further enhancing physiological p-tau and OA-induced tau hyperphosphorylation at CP13 (-OA: -51%,+OA:-12%), RZ3 (-OA:-63%,+OA:-22%), PHF-1 (-OA:-22%,+OA:-13%), AT8 (-OA:-64%,+OA:-5%), AT270 (-OA:-

bioRxiv preprint doi: https://doi.org/10.1101/821389; this version posted October 28, 2019. The copyright holder for this preprint (which was not certified by peer review) is the author/funder, who has granted bioRxiv a license to display the preprint in perpetuity. It is made available under aCC-BY 4.0 International license.

68%,+OA:-63%), and total tau DA31 (-OA:-73%,+OA:-69%)(**Figure 4a, 4b, lane 5 and Figure 5a, 5b, lane 6; Table 4**). β-actin protein levels remained even in all experimental conditions. When samples were probed with αII-spectrin antibody, with the calpain and caspase-3 inhibitors added (S and Z), SBDP150/145 and SBDP120 bands were statistically non-significant compared to control, in both basal and OA-induced tau hyperphosphorylation, suggesting a healthy neuronal culture.

Taken all together, treatments with CKII inhibitor TBB, GSK3 inhibitors LiCl and AR, and Src/Fyn Kinase inhibitor Saracatinib showed robust inhibition leading to different reduced basal and OA-induced tau phosphorylation profiles demonstrating the specificity of inhibitors tested in our tauopathy cell-based models. Thus, the kinase inhibitors studied provide targets to reduce or prevent tau hyperphosphorylation and aggregation in tauopathies.

Discussion

In the present study, OA was used to induce tau hyperphosphorylation and oligomerization in mouse neuroblastoma N2a culture and rat primary cerebrocortical neuronal cultures (CTX) to screen for various tau kinase inhibitors as potential drug candidates. The N2a neuronal cultures have been widely used to study mechanisms of neurodegeneration because they are a homogenous culture system that is convenient to handle and can multiply quickly to produce a tremendous amount of neuron precursor cells (72). However, the primary cultures were implemented in this study as they represent a healthier form of cortical neurons as opposed to cell lines which are cancerous, in a sense that gene expression in primary cortical culture could represent and mimic the actual *in vivo* expression. Additionally, primary culture has the advantage in portraying the complexity of the central nervous system by better translating into *in vivo* models used for

bioRxiv preprint doi: https://doi.org/10.1101/821389; this version posted October 28, 2019. The copyright holder for this preprint (which was not certified by peer review) is the author/funder, who has granted bioRxiv a license to display the preprint in perpetuity. It is made available under aCC-BY 4.0 International license.

509 screening pharmaceutical drug candidate's compounds (73). It has been reported that OA results
510 in robust tau hyperphosphorylation at multiple pathological epitopes in animal and cell culture
511 studies (38, 40, 41, 74-76).

512 OA treatment was used to induce tau hyperphosphorylation and oligomerization at various
513 phospho-tau epitopes in N2a cell culture as a tauopathy model. OA caused down-regulation of
514 protein phosphatase and showed the appearance of oligomeric forms of p-tau species (110 kDa,
515 170 kDa, and 240 kDa) immunoreactive to p-tau-specific antibodies (pSer202, pSer396/404) and
516 total anti-tau (a.a. 102-142). Although the exact mechanism of tauopathy-induced disorders is not
517 yet elucidated, the immunostaining of autopsy brains with anti-p-tau antibodies, including AT8
518 (pSer202/pThr205), and PHF-1 (pSer396/pSer404) are utilized as a diagnostic method of AD and
519 tauopathy (77). Thus, in our study, the increase in tau phosphorylation detected was identified at
520 these sites as a representation of a tauopathy model.

521 Moreover, among all the phospho-tau epitopes studied here, Thr231 epitope is thought to
522 be associated in the initiation of tau hyperphosphorylation in tauopathies while other epitopes such
523 as Thr181, Ser202/Thr205, and Ser396/Ser404 are phosphorylated far ahead during the tauopathy
524 process and the progression of the disease (78). The phosphorylation sites Thr231 and Thr181 have
525 been proposed as biomarkers in AD while Ser202/Thr205 are used to determine the stage of AD
526 progression (79-81). These phosphorylation sites were selected in our study to associate the
527 effectiveness of protein kinase inhibitors with tauopathy-relevant phosphorylation sites.

528 It is widely established that PP2A is the primary enzyme responsible for dephosphorylation
529 of tau protein throughout the brain, controlling all tau phosphorylation sites. PP2A activity is
530 decreased in AD and TBI brains (12, 82). Therefore, the OA-induced inhibition of PP2A is a highly

bioRxiv preprint doi: https://doi.org/10.1101/821389; this version posted October 28, 2019. The copyright holder for this preprint (which was not certified by peer review) is the author/funder, who has granted bioRxiv a license to display the preprint in perpetuity. It is made available under aCC-BY 4.0 International license.

relevant model to study various tau protein kinase inhibitors as modulators of tau hyperphosphorylation and oligomerization targeting tau pathology **(Figure 6, Table 2)**.

In contrast to N2a cell culture, the monomeric form of tau (ranging from 63 kDa – 67 kDa) was only observed in CTX culture. OA might be able to cause tau oligomerization inducing phosphorylation at different sites on tau depending upon the cell line. One possible reason for such effect would be that our separation of tau protein by SDS-PAGE was carried out under reducing conditions (Dithiothreitol (DTT) and β-ME) that could have the ability to minimize tau oligomers to the monomeric form, specifically in CTX primary culture. Our CTX serum-free neurobasal media contained antioxidants such as glutathione. Thus, the addition of these antioxidants may have blocked the process of tau oligomerization from occurring.

In the N2a and CTX cell culture, TBB (CKII inhibitor) surprisingly provided the most profound reversal of tau phosphorylation and oligomerization at the epitopes pSer202, (CP13), pSer396/pSer404 (PHF-1), pSer202/pThr205 (AT8), pThr181 (AT8), and pThr231 (RZ3). TBB is a selective, cell-permeable, ATP/GTP-competitive inhibitor of casein kinase II (CKII) (IC_{50}=900 nM for rat liver) (83). It has been shown that CKII function is aberrant in AD, and its alteration precedes hyperphosphorylated tau accumulation in NFT formation (18). Moreover, it has been reported that CKII can phosphorylate tau purified from human brain and neuroblastoma cell line (18, 83-85). A study has shown that CKII phosphorylates SET, a potent PP2A inhibitor, inducing tau hyperphosphorylation in neurons and animal models, while inhibition of CKII by TBB eliminated this event (86). Thus, inhibition of CKII by TBB might provide a pharmacological interference for treating tauopathy-related disorders.

Since GSK-3 is a well-known kinase that can phosphorylate tau *in vitro* and *in vivo* and has been proposed as a target for pharmacological intervention (87, 88), three GSK-3 small

bioRxiv preprint doi: https://doi.org/10.1101/821389; this version posted October 28, 2019. The copyright holder for this preprint (which was not certified by peer review) is the author/funder, who has granted bioRxiv a license to display the preprint in perpetuity. It is made available under aCC-BY 4.0 International license.

554 molecule kinase inhibitors (LiCl, AR, and A-107) were selected to be assessed on OA-induced
555 tauopathy, cell-based model. AR provided robust suppression of tau hyperphosphorylation in CTX
556 culture at all tau epitopes tested **(Figure 4a, 4b, and Figure 5a, 5b; and Table 4)** and was less
557 effective in N2a cells **(Figure 2a, 2b, and Table 3)**. It was also observed that the effect of AR is
558 more prominent compared to another GSK3 inhibitor, A-107 in CTX primary culture. This effect
559 could be attributed, in part, to the high selectivity and specificity of AR to GSK3β (89) compared
560 to A-107. A-107 display selectivity for both GSK3α and GSK3β (K_i= 0.6 nM for both) (90) thereby
561 might dilute the effect of inhibition of GSK3β, which is regarded as the critical kinase in AD (88).
562 Similarly, a study has shown that hypothermia-induced tau hyperphosphorylation was
563 reduced with AR treatment in human neuroblastoma SH-SY5Y 3R-Tau (76). In another study, AR
564 protected N2a cell culture against apoptosis by inhibition of the phosphatidylinositol-3
565 kinase/protein kinase B pathway and showed neuroprotective properties against neurotoxicity
566 caused by the β-amyloid peptide in hippocampal slices (91). The lack of AR effect on N2a culture
567 might be attributed to differences in cellular mechanisms from CTX culture, mediating OA-
568 induced tau phosphorylation at multiple levels and different sites.
569 LiCl is well-known to inhibit GSK3 and other kinases (76). In CTX culture, LiCl caused
570 dramatic inhibition of basal and OA-induced tau hyperphosphorylation at all tested tau epitopes.
571 Consistent with previous reports, LiCl was shown to reduce tau phosphorylation in cultured cells,
572 Ex-vivo rat brain slices, and rat brains at different AD-related tau epitopes (58, 76, 89, 92-94).
573 Unexpectedly, LiCl showed an opposite impact on N2a culture by increasing OA-induced tau
574 hyperphosphorylation and oligomerization at multiple tested tau epitopes. To the best of our
575 knowledge, this effect is reported herein for the first time in cell culture. However, there are
576 biological targets for LiCl that might have resulted in an adverse event. For instance, one

bioRxiv preprint doi: https://doi.org/10.1101/821389; this version posted October 28, 2019. The copyright holder for this preprint (which was not certified by peer review) is the author/funder, who has granted bioRxiv a license to display the preprint in perpetuity. It is made available under aCC-BY 4.0 International license.

577 hypothesis states that LiCl is a competitive inhibitor of GSK-3 to Mg^{2+}, but not competitive to the
578 substrate or ATP. Another theory proposes that LiCl causes potassium deprivation (95).

579 The use of CDK5 inhibitor Roscovitine in CTX culture substantially reduced basal and
580 OA-induced tau hyperphosphorylation at CP13 (pSer202), RZ3 (pT231, PHF-1(pSer396/pSer404)
581 and AT270 (pThr181). Roscovitine reduced basal phosphorylation at AT8 (pSer202/pThr205) but
582 did not affect the OA-induced tau hyperphosphorylation, reflecting its specificity and the
583 selectivity to our cell models. Similarly, several recent studies revealed that inhibiting CDK5 with
584 Roscovitine had neuroprotective properties against neurodegenerative conditions caused by
585 decreasing tau phosphorylation (66, 76, 96). Like LiCl, Roscovitine resulted in opposite effects in
586 the N2a cells by increasing phosphorylation at CP13 (pSer202) and PHF-1 (pSer396/pSer404).

587 Another protein kinase that has recently received consideration as a pharmaceutical target
588 is the tyrosine kinase Fyn, which has been linked with the amyloid pathway and tau
589 phosphorylation through the N-terminal domain in dendrites (16). Saracatinib (also known as
590 AZD0530) is a small molecular inhibitor that has high potency for Src and Fyn kinases (16, 19-
591 21). Fyn can physically associate with tau and phosphorylate residues by interacting through its
592 SH3 domain with SH3-binding domains in tau **(Figure 6)** (97). In our experiments, Saracatinib
593 reduced both basal and OA-induced tau hyperphosphorylation (67 kDa) in N2a and CTX primary
594 cultures at the epitopes: CP13 (pSer202), RZ3 (pThr231), PHF-1 (pSer396/pSer404) and AT270
595 (pThr181). Saracatinib did not affect the pSer202/pThr205 (AT8) site, suggesting that Fyn does
596 not phosphorylate Thr205 residue in our experimental tauopathy model.

597 Cyclosporine (CsA) or FK506 is an 11 amino acid cyclic non-ribosomal peptide used as
598 an immunosuppressant. CsA is known to induce neuroprotective properties through inhibiting
599 specifically enzyme activity by binding to cyclophilin, forming a complex that inhibits calcineurin

bioRxiv preprint doi: https://doi.org/10.1101/821389; this version posted October 28, 2019. The copyright holder for this preprint (which was not certified by peer review) is the author/funder, who has granted bioRxiv a license to display the preprint in perpetuity. It is made available under aCC-BY 4.0 International license.

(PP3) (98) **(Figure 6, Table 2).** Several findings have shown that calcineurin inhibition increases tau hyperphosphorylation, and cells treated with CsA could induce the process (99, 100). In the present study, it was found that treatment with CsA alone did not result in any significant increase in tau levels or tau phosphorylation, which lies in agreement with a study done similarly (101), and reported complete inhibition of OA-induced tau hyperphosphorylation and oligomerization in N2a cells at the examined tau epitopes. In CTX culture, CsA produced a lower but still considerable reduction of OA-induced tau phosphorylation compared to N2a neuronal culture. These data suggest that PP2A is the main enzyme that regulates tau dephosphorylation in our culture system rather than PP3 at the tested sites. Moreover, we propose that CsA inhibits PP3 by blocking its binding to the calcium-dependent calmodulin, required for CaMKII to be active, thereby decreasing tau hyperphosphorylation **(Figure 6, Table 2)**.

Conclusions

In this study, OA was used to induce tauopathy in neuroblastoma and differentiated neuronal culture and screen for various pharmaceutical drug candidates. We provided a side-by-side comparison of possible drug candidates that are well described in respect to tauopathies such as Alzheimer's (Saracatinib, LiCl, AR) as well as other prospects which have been minimally studied in application to potential therapies (TBB and CsA). TBB and CsA warrant further test design involving an animal model of tauopathy. This is particularly important as recent studies implicate pre-fibrillar hyperphosphorylated tau as the toxic species in AD, CTE, and other neurodegenerative diseases, therefore, re-establishing the interest in tau kinase inhibitors development at putative neurotherapies, which could translate into human clinical trials.

Limitation and Future Directions

bioRxiv preprint doi: https://doi.org/10.1101/821389; this version posted October 28, 2019. The copyright holder for this preprint (which was not certified by peer review) is the author/funder, who has granted bioRxiv a license to display the preprint in perpetuity. It is made available under aCC-BY 4.0 International license.

623 With the use of peptidomic, it is evident that unique peptides are the main causes of
624 tauopathies; we hypothesized that after using OA induced tau hyperphosphorylation as a tauopathy
625 model, different drugs could be tested as neurotherapeutic targets for tauopathies-related disorders.
626 In one study, different Kinase inhibitors were tested on samples, to model possible therapeutic
627 drugs. TBB is a novel CKII inhibitor that has not been used for tauopathies and can be an example
628 for other possible drugs.
629
630 The idea of targeting specific biomarkers, after Peptidomic screening helped identified
631 potential kinase inhibitor candidates (AR, TBB, CsA, and Saracatinib) that warrant further test
632 design. The study would like to further test this protocol on 3R vs 4R human tau cell cultures.
633 Experiments on CSF and blood samples are being run to make up for the high based evidence on
634 rodent cultures.
635
636 Some limitations to the study include the idea that these compound dilutions are arbitrary
637 or based on references using different cell systems. Treatment is often in the high micromolar
638 range where compounds acts on more than their primary target. The use of serial dilution and the
639 generation of an EC50 would have been more appropriate.
640
641 Furthermore, the technic used is entirely based on western blotting which prohibits its
642 potential use in higher throughput screens. These systems are highly specific, but a wider variety
643 of auto-antibody assays, would have provided more accurate results.
644

bioRxiv preprint doi: https://doi.org/10.1101/821389; this version posted October 28, 2019. The copyright holder for this preprint (which was not certified by peer review) is the author/funder, who has granted bioRxiv a license to display the preprint in perpetuity. It is made available under aCC-BY 4.0 International license.

Finally, one constraint to this study remain from a lack of interpretation on why some compounds respond in basal conditions while other respond in OA-treated conditions. The discrepancy in response between the N2a cell line and CTX also cautions the interpretation of the screen. Having a wider variety of samples from different parts of the brain, could have potentially given more precise evidence toward the study.

List of Abbreviations

(A-1070722)	1-(7-methoxyquinolin-4-yl)-3-(6-(trifluoromethyl) pyridin-2-yl
AD	Alzheimer's disease
AR-A014418	N-(4-methoxybenzyl)-N'-(5-nitro-1,3-thiazol-2-yl) urea
AZD0530	Saracatinib
BCIT/NBT	5-bromo-4-chloro- 3-indolyl phosphate
CaMKII	Ca^{2+}/calmodulin-dependent protein kinase II
CDK5	Cyclin-dependent kinase 5
CK2	Casein kinase
CKII	Casein kinase II
CsA	Cyclosporin A
CTE	Chronic traumatic encephalopathy
CTX	Neuronal cortical cell cultures
DTT	Dithiothreitol
DYRK1A/2	Dual-specificity tyrosine kinase phosphorylation and regulated kinase-1A/2

bioRxiv preprint doi: https://doi.org/10.1101/821389; this version posted October 28, 2019. The copyright holder for this preprint (which was not certified by peer review) is the author/funder, who has granted bioRxiv a license to display the preprint in perpetuity. It is made available under aCC-BY 4.0 International license.

EGTA	Ethylene glycol-bis (β-aminoethyl ether)-N,N,N',N'-tetraacetic acid
GSK-3	Glycogen synthase kinase 3 inhibitors
HMW	High Molecular Weight
K252a	Staurosporine analog, non-selective cell permeable Protein Kinase Inhibitor; (9S,10R,12R)-2,3,9,10,11,12-Hexahydro-10-hydroxy-9-methyl-1-oxo-9,12-epoxy-1H-diindolo[1,2,3-fg:3',2',1'-kl]pyrrolo[3,4-i][1,6]benzodiazocine-10-carboxylic acid methyl ester
LiCl	Lithium Chloride
LMW-MT	Low molecular weight monomeric tau
MLCK	Myosin light-chain kinase
N2A	Neuroblastoma cell line
NFT	Neurofibrillary tangles
NMDAR	N-methyl-D-aspartate receptors
OA	Okadaic acid
PP1	Protein Phosphatase 1
PP2A	Protein Phosphatase 2A
Roscovitine	(2R)-2-1-butanol

bioRxiv preprint doi: https://doi.org/10.1101/821389; this version posted October 28, 2019. The copyright holder for this preprint (which was not certified by peer review) is the author/funder, who has granted bioRxiv a license to display the preprint in perpetuity. It is made available under aCC-BY 4.0 International license.

Saracatinib	N-(5-chloro-1,3-benzodioxol-4-yl)-7-[2-(4-methylpiperazin-1-yl)ethoxy]-5-(tetrahydro-2H-pyran-4-yloxy)quinazolin-4-amine
SBDP	Spectrin breakdown products
SNJ-1945	Amphipathic ketoamide
STS	Staurosporine; (5S,6R,7R,9R)-6-methoxy-5-methyl-7-(methylamino)-6,7,8,9,15,16-hexahydro-17-oxa-4b,9a,15-triaza-5,9-methanodibenzo[b,h]cyclonona[jkl]cyclopenta[e]-as-indacen-14(5h)-one
TBB	4,5,6,7-tetrabromobenzotriazole
Z-DCB	Caspase-3; Z-Asp-2,6-Dichlorobenzoyloxymethyl Ketone

Declarations

Availability of data and material

- All data generated or analyzed during this study are included in this article (and its additional files).

Competing interests

- The authors declare that they have no conflict of interest.

Funding

bioRxiv preprint doi: https://doi.org/10.1101/821389; this version posted October 28, 2019. The copyright holder for this preprint (which was not certified by peer review) is the author/funder, who has granted bioRxiv a license to display the preprint in perpetuity. It is made available under aCC-BY 4.0 International license.

660 • This work was supported by funding from the University of Florida Departments of
661 Emergency Medicine and Psychiatry.

662 **Authors' contributions**

663 Conceived and designed the experiments: HY, KW. Performed the experiments: HY, IT, GA, MK.
664 Analyzed the Data: HY, KW. Contributed reagents/material/analysis tools: ZY, FL, and PD.
665 Performed revision experiments: HY and KW. Wrote the manuscript: HY, MK Reviewed the
666 manuscript: RY, KW, and FK.

667 **Acknowledgment**

668 We would like to thank Dr. Peter Davies (Albert Einstein College of Medicine, Bronx, NY, USA)
669 for the kind gift of monoclonal tau antibodies.

670

671

672

673

674

675

676

bioRxiv preprint doi: https://doi.org/10.1101/821389; this version posted October 28, 2019. The copyright holder for this preprint (which was not certified by peer review) is the author/funder, who has granted bioRxiv a license to display the preprint in perpetuity. It is made available under aCC-BY 4.0 International license.

677

678 ## References

679 1. Sparks P, Lawrence T, Hinze S. Neuroimaging in the Diagnosis of Chronic Traumatic
680 Encephalopathy: A Systematic Review. Clin J Sport Med. 2017.
681 2. Panza F, Imbimbo BP, Lozupone M, Greco A, Seripa D, Logroscino G, et al. Disease-modifying
682 therapies for tauopathies: agents in the pipeline. Expert Rev Neurother. 2019.
683 3. Mohamed AZ, Cumming P, Gotz J, Nasrallah F, Department of Defense Alzheimer's Disease
684 Neuroimaging I. Tauopathy in veterans with long-term posttraumatic stress disorder and traumatic brain
685 injury. Eur J Nucl Med Mol Imaging. 2019;46(5):1139-51.
686 4. Wang L, Benzinger TL, Su Y, Christensen J, Friedrichsen K, Aldea P, et al. Evaluation of Tau Imaging
687 in Staging Alzheimer Disease and Revealing Interactions Between beta-Amyloid and Tauopathy. JAMA
688 Neurol. 2016;73(9):1070-7.
689 5. Besser LM, Mock C, Teylan MA, Hassenstab J, Kukull WA, Crary JF. Differences in Cognitive
690 Impairment in Primary Age-Related Tauopathy Versus Alzheimer Disease. J Neuropathol Exp Neurol. 2019.
691 6. Pir GJ, Choudhary B, Mandelkow E. models of tauopathy. FASEB J. 2017;31(12):5137-48.
692 7. Perrine K, Helcer J, Tsiouris AJ, Pisapia DJ, Stieg P. The Current Status of Research on Chronic
693 Traumatic Encephalopathy. World Neurosurg. 2017;102:533-44.
694 8. Kovacs GG. Tauopathies. Handb Clin Neurol. 2017;145:355-68.
695 9. Neve RL, Harris P, Kosik KS, Kurnit DM, Donlon TA. Identification of cDNA clones for the human
696 microtubule-associated protein tau and chromosomal localization of the genes for tau and microtubule-
697 associated protein 2. Brain Res. 1986;387(3):271-80.
698 10. Avila J, Jiménez JS, Sayas CL, Bolós M, Zabala JC, Rivas G, et al. Tau Structures. Front Aging
699 Neurosci. 2016;8:262.
700 11. Lee G, Leugers CJ. Tau and Tauopathies. Prog Mol Biol Transl Sci. 2012;107:263-93.
701 12. Theendakara V, Bredesen DE, Rao RV. Downregulation of protein phosphatase 2A by
702 apolipoprotein E: Implications for Alzheimer's disease. Mol Cell Neurosci. 2017;83:83-91.
703 13. Stoothoff WH, Johnson GV. Tau phosphorylation: physiological and pathological consequences.
704 Biochim Biophys Acta. 2005;1739(2-3):280-97.
705 14. Ni R, Ji B, Ono M, Sahara N, Zhang MR, Aoki I, et al. Comparative in-vitro and in-vivo quantifications
706 of pathological tau deposits and their association with neurodegeneration in tauopathy mouse models. J
707 Nucl Med. 2018.
708 15. Sahara N, Shimojo M, Ono M, Takuwa H, Febo M, Higuchi M, et al. Tau Imaging for a Diagnostic
709 Platform of Tauopathy Using the rTg4510 Mouse Line. Front Neurol. 2017;8:663.
710 16. Nygaard HB. Targeting Fyn Kinase in Alzheimer's Disease. Biol Psychiatry. 2018;83(4):369-76.
711 17. Martin L, Latypova X, Wilson CM, Magnaudeix A, Perrin ML, Yardin C, et al. Tau protein kinases:
712 involvement in Alzheimer's disease. Ageing Res Rev. 2013;12(1):289-309.
713 18. Rosenberger AF, Morrema TH, Gerritsen WH, van Haastert ES, Snkhchyan H, Hilhorst R, et al.
714 Increased occurrence of protein kinase CK2 in astrocytes in Alzheimer's disease pathology. J
715 Neuroinflammation. 2016;13:4.
716 19. Li C, Götz J. Somatodendritic accumulation of Tau in Alzheimer's disease is promoted by Fyn-
717 mediated local protein translation. EMBO J. 2017;36(21):3120-38.
718 20. Liu W, Zhao J, Lu G. miR-106b inhibits tau phosphorylation at Tyr18 by targeting Fyn in a model of
719 Alzheimer's disease. Biochem Biophys Res Commun. 2016;478(2):852-7.
720 21. Kaufman AC, Salazar SV, Haas LT, Yang J, Kostylev MA, Jeng AT, et al. Fyn inhibition rescues
721 established memory and synapse loss in Alzheimer mice. Ann Neurol. 2015;77(6):953-71.

bioRxiv preprint doi: https://doi.org/10.1101/821389; this version posted October 28, 2019. The copyright holder for this preprint (which was not certified by peer review) is the author/funder, who has granted bioRxiv a license to display the preprint in perpetuity. It is made available under aCC-BY 4.0 International license.

22. Dolan PJ, Johnson GV. The role of tau kinases in Alzheimer's disease. Curr Opin Drug Discov Devel. 2010;13(5):595-603.
23. Bennett PC, Zhao W, Ng KT. Concentration-dependent effects of protein phosphatase (PP) inhibitors implicate PP1 and PP2A in different stages of memory formation. Neurobiol Learn Mem. 2001;75(1):91-110.
24. Ando K, Maruko-Otake A, Ohtake Y, Hayashishita M, Sekiya M, Iijima KM. Stabilization of Microtubule-Unbound Tau via Tau Phosphorylation at Ser262/356 by Par-1/MARK Contributes to Augmentation of AD-Related Phosphorylation and Abeta42-Induced Tau Toxicity. PLoS Genet. 2016;12(3):e1005917.
25. Gerson JE, Farmer KM, Henson N, Castillo-Carranza DL, Carretero Murillo M, Sengupta U, et al. Tau oligomers mediate alpha-synuclein toxicity and can be targeted by immunotherapy. Mol Neurodegener. 2018;13(1):13.
26. Tan CC, Zhang XY, Tan L, Yu JT. Tauopathies: Mechanisms and Therapeutic Strategies. J Alzheimers Dis. 2018;61(2):487-508.
27. Wang KK, Yang Z, Zhu T, Shi Y, Rubenstein R, Tyndall JA, et al. An update on diagnostic and prognostic biomarkers for traumatic brain injury. Expert Rev Mol Diagn. 2018;18(2):165-80.
28. Aldag M, Armstrong RC, Bandak F, Bellgowan PSF, Bentley T, Biggerstaff S, et al. The Biological Basis of Chronic Traumatic Encephalopathy following Blast Injury: A Literature Review. J Neurotrauma. 2017;34(S1):S26-S43.
29. Panza F, Solfrizzi V, Seripa D, Imbimbo BP, Lozupone M, Santamato A, et al. Tau-based therapeutics for Alzheimer's disease: active and passive immunotherapy. Immunotherapy. 2016;8(9):1119-34.
30. Tolosa E, Litvan I, Höglinger GU, Burn D, Lees A, Andrés MV, et al. A phase 2 trial of the GSK-3 inhibitor tideglusib in progressive supranuclear palsy. Mov Disord. 2014;29(4):470-8.
31. Georgievska B, Sandin J, Doherty J, Mörtberg A, Neelissen J, Andersson A, et al. AZD1080, a novel GSK3 inhibitor, rescues synaptic plasticity deficits in rodent brain and exhibits peripheral target engagement in humans. J Neurochem. 2013;125(3):446-56.
32. Ludolph AC, Kassubek J, Landwehrmeyer BG, Mandelkow E, Mandelkow EM, Burn DJ, et al. Tauopathies with parkinsonism: clinical spectrum, neuropathologic basis, biological markers, and treatment options. Eur J Neurol. 2009;16(3):297-309.
33. Medina M. An Overview on the Clinical Development of Tau-Based Therapeutics. Int J Mol Sci. 2018;19(4).
34. Tell V, Hilgeroth A. Recent developments of protein kinase inhibitors as potential AD therapeutics. Front Cell Neurosci. 2013;7:189.
35. Alonso AD, Di Clerico J, Li B, Corbo CP, Alaniz ME, Grundke-Iqbal I, et al. Phosphorylation of tau at Thr212, Thr231, and Ser262 combined causes neurodegeneration. J Biol Chem. 2010;285(40):30851-60.
36. Simic G, Babic Leko M, Wray S, Harrington C, Delalle I, Jovanov-Milosevic N, et al. Tau Protein Hyperphosphorylation and Aggregation in Alzheimer's Disease and Other Tauopathies, and Possible Neuroprotective Strategies. Biomolecules. 2016;6(1):6.
37. Rabano A, Cuadros R, Merino-Serrais P, Rodal I, Benavides-Piccione R, Gomez E, et al. Protocols for Monitoring the Development of Tau Pathology in Alzheimer's Disease. Methods Mol Biol. 2016;1303:143-60.
38. Kamat PK, Rai S, Swarnkar S, Shukla R, Ali S, Najmi AK, et al. Okadaic acid-induced Tau phosphorylation in rat brain: role of NMDA receptor. Neuroscience. 2013;238:97-113.
39. Ho YS, Yang X, Lau JC, Hung CH, Wuwongse S, Zhang Q, et al. Endoplasmic reticulum stress induces tau pathology and forms a vicious cycle: implication in Alzheimer's disease pathogenesis. J Alzheimers Dis. 2012;28(4):839-54.

bioRxiv preprint doi: https://doi.org/10.1101/821389; this version posted October 28, 2019. The copyright holder for this preprint (which was not certified by peer review) is the author/funder, who has granted bioRxiv a license to display the preprint in perpetuity. It is made available under aCC-BY 4.0 International license.

40. Jones NC, Nguyen T, Corcoran NM, Velakoulis D, Chen T, Grundy R, et al. Targeting hyperphosphorylated tau with sodium selenate suppresses seizures in rodent models. Neurobiol Dis. 2012;45(3):897-901.
41. Broetto N, Hansen F, Brolese G, Batassini C, Lirio F, Galland F, et al. Intracerebroventricular administration of okadaic acid induces hippocampal glucose uptake dysfunction and tau phosphorylation. Brain Res Bull. 2016;124:136-43.
42. Wang J, Tung YC, Wang Y, Li XT, Iqbal K, Grundke-Iqbal I. Hyperphosphorylation and accumulation of neurofilament proteins in Alzheimer disease brain and in okadaic acid-treated SY5Y cells. FEBS Lett. 2001;507(1):81-7.
43. Baker S, Gotz J. A local insult of okadaic acid in wild-type mice induces tau phosphorylation and protein aggregation in anatomically distinct brain regions. Acta neuropathologica communications. 2016;4:32.
44. Boban M, Babic Leko M, Miskic T, Hof PR, Simic G. Human neuroblastoma SH-SY5Y cells treated with okadaic acid express phosphorylated high molecular weight tau-immunoreactive protein species. J Neurosci Methods. 2019;319:60-8.
45. Shen XY, Luo T, Li S, Ting OY, He F, Xu J, et al. Quercetin inhibits okadaic acid-induced tau protein hyperphosphorylation through the Ca2+‐calpain‐p25‐CDK5 pathway in HT22 cells. Int J Mol Med. 2018;41(2):1138-46.
46. Zhang Z, Simpkins JW. An okadaic acid-induced model of tauopathy and cognitive deficiency. Brain Res. 2010;1359:233-46.
47. Valdiglesias V, Prego-Faraldo MV, Pasaro E, Mendez J, Laffon B. Okadaic acid: more than a diarrheic toxin. Mar Drugs. 2013;11(11):4328-49.
48. Koumura A, Nonaka Y, Hyakkoku K, Oka T, Shimazawa M, Hozumi I, et al. A novel calpain inhibitor, ((1S)-1((((1S)-1-benzyl-3-cyclopropylamino-2,3-di-oxopropyl)amino)carbonyl)-3-methylbutyl) carbamic acid 5-methoxy-3-oxapentyl ester, protects neuronal cells from cerebral ischemia-induced damage in mice. Neuroscience. 2008;157(2):309-18.
49. Drognitz O, Obermaier R, Liu X, Neeff H, von Dobschuetz E, Hopt UT, et al. Effects of organ preservation, ischemia time and caspase inhibition on apoptosis and microcirculation in rat pancreas transplantation. Am J Transplant. 2004;4(7):1042-50.
50. Kobeissy FH, Liu MC, Yang Z, Zhang Z, Zheng W, Glushakova O, et al. Degradation of betaII-Spectrin Protein by Calpain-2 and Caspase-3 Under Neurotoxic and Traumatic Brain Injury Conditions. Mol Neurobiol. 2015;52(1):696-709.
51. Mondello S, Robicsek SA, Gabrielli A, Brophy GM, Papa L, Tepas J, et al. αII-Spectrin Breakdown Products (SBDPs): Diagnosis and Outcome in Severe Traumatic Brain Injury Patients. J Neurotrauma. 2010;27(7):1203-13.
52. Khélifa T, Beck WT. Induction of apoptosis by dexrazoxane (ICRF-187) through caspases in the absence of c-jun expression and c-Jun NH2-terminal kinase 1 (JNK1) activation in VM-26-resistant CEM cells. Biochem Pharmacol. 1999;58(8):1247-57.
53. Iimoto DS, Masliah E, DeTeresa R, Terry RD, Saitoh T. Aberrant casein kinase II in Alzheimer's disease. Brain Res. 1990;507(2):273-80.
54. Toledo FD, Pérez LM, Basiglio CL, Ochoa JE, Sanchez Pozzi EJ, Roma MG. The Ca^{2+}-calmodulin-Ca^{2+}/calmodulin-dependent protein kinase II signaling pathway is involved in oxidative stress-induced mitochondrial permeability transition and apoptosis in isolated rat hepatocytes. Arch Toxicol. 2014;88(9):1695-709.
55. Iqbal K, Liu F, Gong CX, Grundke-Iqbal I. Tau in Alzheimer Disease and Related Tauopathies. Curr Alzheimer Res. 2010;7(8):656-64.
56. Qin N, Olcese R, Bransby M, Lin T, Birnbaumer L. Ca2+-induced inhibition of the cardiac Ca2+ channel depends on calmodulin. Proc Natl Acad Sci U S A. 1999;96(5):2435-8.

bioRxiv preprint doi: https://doi.org/10.1101/821389; this version posted October 28, 2019. The copyright holder for this preprint (which was not certified by peer review) is the author/funder, who has granted bioRxiv a license to display the preprint in perpetuity. It is made available under aCC-BY 4.0 International license.

817 57. Song JS, Yang SD. Tau protein kinase I/GSK-3 beta/kinase FA in heparin phosphorylates tau on
818 Ser199, Thr231, Ser235, Ser262, Ser369, and Ser400 sites phosphorylated in Alzheimer disease brain. J
819 Protein Chem. 1995;14(2):95-105.
820 58. Noble W, Planel E, Zehr C, Olm V, Meyerson J, Suleman F, et al. Inhibition of glycogen synthase
821 kinase-3 by lithium correlates with reduced tauopathy and degeneration in vivo. Proc Natl Acad Sci U S A.
822 2005;102(19):6990-5.
823 59. Prabhakaran J, Zanderigo F, Solingapuram Sai KK, Rubin-Falcone H, Jorgensen MJ, Kaplan JR, et al.
824 Radiosynthesis and in Vivo Evaluation of [11C]A1070722, a High Affinity GSK-3 PET Tracer in Primate Brain.
825 ACS Chem Neurosci. 2017;8(8):1697-703.
826 60. Gucalp A, Sparano JA, Caravelli J, Santamauro J, Patil S, Abbruzzi A, et al. Phase II trial of saracatinib
827 (AZD0530), an oral SRC-inhibitor for the treatment of patients with hormone receptor-negative metastatic
828 breast cancer. Clin Breast Cancer. 2011;11(5):306-11.
829 61. Tapley P, Lamballe F, Barbacid M. K252a is a selective inhibitor of the tyrosine protein kinase
830 activity of the trk family of oncogenes and neurotrophin receptors. Oncogene. 1992;7(2):371-81.
831 62. Zimmermann A, Keller H. Effects of staurosporine, K 252a and other structurally related protein
832 kinase inhibitors on shape and locomotion of Walker carcinosarcoma cells. Br J Cancer. 1992;66(6):1077-
833 82.
834 63. Ruegg UT, Burgess GM. Staurosporine, K-252 and UCN-01: potent but nonspecific inhibitors of
835 protein kinases. Trends in pharmacological sciences. 1989;10(6):218-20.
836 64. Liu MC, Kobeissy F, Zheng W, Zhang Z, Hayes RL, Wang KK. Dual vulnerability of tau to calpains
837 and caspase-3 proteolysis under neurotoxic and neurodegenerative conditions. ASN Neuro.
838 2011;3(1):e00051.
839 65. Wang KK, Yang Z, Chiu A, Lin F, Rubenstein R. Examining the Neural and Astroglial Protective
840 Effects of Cellular Prion Protein Expression and Cell Death Protease Inhibition in Mouse Cerebrocortical
841 Mixed Cultures. Mol Neurobiol. 2016;53(7):4821-32.
842 66. Meijer L, Borgne A, Mulner O, Chong JP, Blow JJ, Inagaki N, et al. Biochemical and cellular effects
843 of roscovitine, a potent and selective inhibitor of the cyclin-dependent kinases cdc2, cdk2 and cdk5.
844 European journal of biochemistry. 1997;243(1-2):527-36.
845 67. Bhounsule AS, Bhatt LK, Prabhavalkar KS, Oza M. Cyclin dependent kinase 5: A novel avenue for
846 Alzheimer's disease. Brain Res Bull. 2017;132:28-38.
847 68. Engmann O, Giese KP. Crosstalk between Cdk5 and GSK3β: Implications for Alzheimer's Disease.
848 Frontiers in Molecular Neuroscience. 2009;2:2.
849 69. Sengupta A, Grundke-Iqbal I, Iqbal K. Regulation of phosphorylation of tau by protein kinases in
850 rat brain. Neurochem Res. 2006;31(12):1473-80.
851 70. Davis DR, Brion JP, Couck AM, Gallo JM, Hanger DP, Ladhani K, et al. The phosphorylation state of
852 the microtubule-associated protein tau as affected by glutamate, colchicine and beta-amyloid in primary
853 rat cortical neuronal cultures. Biochem J. 1995;309 (Pt 3):941-9.
854 71. Sahara N, DeTure M, Ren Y, Ebrahim AS, Kang D, Knight J, et al. Characteristics of TBS-extractable
855 hyperphosphorylated tau species: aggregation intermediates in rTg4510 mouse brain. J Alzheimers Dis.
856 2013;33(1):249-63.
857 72. Chen Y, Wang C, Hu M, Pan J, Chen J, Duan P, et al. Effects of ginkgolide A on okadaic acid-induced
858 tau hyperphosphorylation and the PI3K-Akt signaling pathway in N2a cells. Planta Med. 2012;78(12):1337-
859 41.
860 73. Schlachetzki JC, Saliba SW, Oliveira AC. Studying neurodegenerative diseases in culture models.
861 Rev Bras Psiquiatr. 2013;35 Suppl 2:S92-100.
862 74. Zhao L, Xiao Y, Wang XL, Pei J, Guan ZZ. Original Research: Influence of okadaic acid on
863 hyperphosphorylation of tau and nicotinic acetylcholine receptors in primary neurons. Exp Biol Med
864 (Maywood). 2016;241(16):1825-33.

bioRxiv preprint doi: https://doi.org/10.1101/821389; this version posted October 28, 2019. The copyright holder for this preprint (which was not certified by peer review) is the author/funder, who has granted bioRxiv a license to display the preprint in perpetuity. It is made available under aCC-BY 4.0 International license.

865 75. Hübinger G, Geis S, LeCorre S, Mühlbacher S, Gordon S, Fracasso RP, et al. Inhibition of PHF-like
866 tau hyperphosphorylation in SH-SY5Y cells and rat brain slices by K252a. J Alzheimers Dis. 2008;13(3):281-
867 94.
868 76. Bretteville A, Marcouiller F, Julien C, El Khoury NB, Petry FR, Poitras I, et al. Hypothermia-induced
869 hyperphosphorylation: a new model to study tau kinase inhibitors. Sci Rep. 2012;2:480.
870 77. Kimura T, Sharma G, Ishiguro K, Hisanaga SI. Phospho-Tau Bar Code: Analysis of Phosphoisotypes
871 of Tau and Its Application to Tauopathy. Front Neurosci. 2018;12:44.
872 78. Augustinack JC, Schneider A, Mandelkow EM, Hyman BT. Specific tau phosphorylation sites
873 correlate with severity of neuronal cytopathology in Alzheimer's disease. Acta Neuropathol.
874 2002;103(1):26-35.
875 79. Hampel H, Buerger K, Zinkowski R, Teipel SJ, Goernitz A, Andreasen N, et al. Measurement of
876 phosphorylated tau epitopes in the differential diagnosis of Alzheimer disease: a comparative
877 cerebrospinal fluid study. Arch Gen Psychiatry. 2004;61(1):95-102.
878 80. Hampel H, Goernitz A, Buerger K. Advances in the development of biomarkers for Alzheimer's
879 disease: from CSF total tau and Abeta(1-42) proteins to phosphorylated tau protein. Brain Res Bull.
880 2003;61(3):243-53.
881 81. Buerger K, Teipel SJ, Zinkowski R, Blennow K, Arai H, Engel R, et al. CSF tau protein phosphorylated
882 at threonine 231 correlates with cognitive decline in MCI subjects. Neurology. 2002;59(4):627-9.
883 82. Lucke-Wold BP, Turner RC, Logsdon AF, Bailes JE, Huber JD, Rosen CL. Linking traumatic brain
884 injury to chronic traumatic encephalopathy: identification of potential mechanisms leading to
885 neurofibrillary tangle development. J Neurotrauma. 2014;31(13):1129-38.
886 83. Sarno S, Papinutto E, Franchin C, Bain J, Elliott M, Meggio F, et al. ATP site-directed inhibitors of
887 protein kinase CK2: an update. Curr Top Med Chem. 2011;11(11):1340-51.
888 84. Avila J, Ulloa L, González J, Moreno F, Díaz-Nido J. Phosphorylation of microtubule-associated
889 proteins by protein kinase CK2 in neuritogenesis. Cell Mol Biol Res. 1994;40(5-6):573-9.
890 85. Greenwood JA, Scott CW, Spreen RC, Caputo CB, Johnson GV. Casein kinase II preferentially
891 phosphorylates human tau isoforms containing an amino-terminal insert. Identification of threonine 39
892 as the primary phosphate acceptor. J Biol Chem. 1994;269(6):4373-80.
893 86. Zhang Q, Xia Y, Wang Y, Shentu Y, Zeng K, Mahaman YAR, et al. CK2 Phosphorylating I2(PP2A)/SET
894 Mediates Tau Pathology and Cognitive Impairment. Front Mol Neurosci. 2018;11:146.
895 87. Medina M, Garrido JJ, Wandosell FG. Modulation of GSK-3 as a Therapeutic Strategy on Tau
896 Pathologies. Front Mol Neurosci. 2011;4:24.
897 88. Llorens-Martin M, Jurado J, Hernandez F, Avila J. GSK-3beta, a pivotal kinase in Alzheimer disease.
898 Front Mol Neurosci. 2014;7:46.
899 89. Gould TD, Einat H, Bhat R, Manji HK. AR-A014418, a selective GSK-3 inhibitor, produces
900 antidepressant-like effects in the forced swim test. Int J Neuropsychopharmacol. 2004;7(4):387-90.
901 90. Prabhakaran J, Zanderigo F, Sai KKS, Rubin-Falcone H, Jorgensen MJ, Kaplan JR, et al.
902 Radiosynthesis and in Vivo Evaluation of [ACS Chem Neurosci. 2017;8(8):1697-703.
903 91. Bhat R, Xue Y, Berg S, Hellberg S, Ormo M, Nilsson Y, et al. Structural insights and biological effects
904 of glycogen synthase kinase 3-specific inhibitor AR-A014418. J Biol Chem. 2003;278(46):45937-45.
905 92. Orena SJ, Torchia AJ, Garofalo RS. Inhibition of glycogen-synthase kinase 3 stimulates glycogen
906 synthase and glucose transport by distinct mechanisms in 3T3-L1 adipocytes. J Biol Chem.
907 2000;275(21):15765-72.
908 93. Fu ZQ, Yang Y, Song J, Jiang Q, Lin ZC, Wang Q, et al. LiCl attenuates thapsigargin-induced tau
909 hyperphosphorylation by inhibiting GSK-3beta in vivo and in vitro. J Alzheimers Dis. 2010;21(4):1107-17.
910 94. Lee S, Shea TB. Regulation of tau proteolysis by phosphatases. Brain Res. 2013;1495:30-6.
911 95. Kramer T, Schmidt B, Lo Monte F. Small-Molecule Inhibitors of GSK-3: Structural Insights and Their
912 Application to Alzheimer's Disease Models. Int J Alzheimers Dis. 2012;2012:381029.

bioRxiv preprint doi: https://doi.org/10.1101/821389; this version posted October 28, 2019. The copyright holder for this preprint (which was not certified by peer review) is the author/funder, who has granted bioRxiv a license to display the preprint in perpetuity. It is made available under aCC-BY 4.0 International license.

913 96. Liu J, Yang J, Xu Y, Guo G, Cai L, Wu H, et al. Roscovitine, a CDK5 Inhibitor, Alleviates Sevoflurane-
914 Induced Cognitive Dysfunction via Regulation Tau/GSK3beta and ERK/PPARgamma/CREB Signaling. Cell
915 Physiol Biochem. 2017;44(2):423-35.
916 97. Polanco JC, Li C, Bodea LG, Martinez-Marmol R, Meunier FA, Gotz J. Amyloid-beta and tau
917 complexity - towards improved biomarkers and targeted therapies. Nat Rev Neurol. 2018;14(1):22-39.
918 98. Liu J, Farmer JD, Jr., Lane WS, Friedman J, Weissman I, Schreiber SL. Calcineurin is a common
919 target of cyclophilin-cyclosporin A and FKBP-FK506 complexes. Cell. 1991;66(4):807-15.
920 99. Wang Q, Wang J. Injection of bradykinin or cyclosporine A to hippocampus induces Alzheimer-like
921 phosphorylation of Tau and abnormal behavior in rats. Chin Med J (Engl). 2002;115(6):884-7.
922 100. Yu DY, Luo J, Bu F, Song GJ, Zhang LQ, Wei Q. Inhibition of calcineurin by infusion of CsA causes
923 hyperphosphorylation of tau and is accompanied by abnormal behavior in mice. Biol Chem.
924 2006;387(7):977-83.
925 101. Gong CX, Lidsky T, Wegiel J, Zuck L, Grundke-Iqbal I, Iqbal K. Phosphorylation of microtubule-
926 associated protein tau is regulated by protein phosphatase 2A in mammalian brain. Implications for
927 neurofibrillary degeneration in Alzheimer's disease. J Biol Chem. 2000;275(8):5535-44.
928 102. Bialojan C, Takai A. Inhibitory effect of a marine-sponge toxin, okadaic acid, on protein
929 phosphatases. Specificity and kinetics. Biochem J. 1988;256(1):283-90.
930 103. Swingle M, Ni L, Honkanen RE. Small-molecule inhibitors of ser/thr protein phosphatases:
931 specificity, use and common forms of abuse. Methods Mol Biol. 2007;365:23-38.
932 104. Amundsen R, Asberg A, Ohm IK, Christensen H. Cyclosporine A- and tacrolimus-mediated
933 inhibition of CYP3A4 and CYP3A5 in vitro. Drug Metab Dispos. 2012;40(4):655-61.
934 105. Serkova N, Brand A, Christians U, Leibfritz D. Evaluation of the effects of immunosuppressants on
935 neuronal and glial cells in vitro by multinuclear magnetic resonance spectroscopy. Biochim Biophys Acta.
936 1996;1314(1-2):93-104.
937 106. Zhang F, Phiel CJ, Spece L, Gurvich N, Klein PS. Inhibitory phosphorylation of glycogen synthase
938 kinase-3 (GSK-3) in response to lithium. Evidence for autoregulation of GSK-3. J Biol Chem.
939 2003;278(35):33067-77.
940 107. Ryves WJ, Harwood AJ. Lithium inhibits glycogen synthase kinase-3 by competition for
941 magnesium. Biochem Biophys Res Commun. 2001;280(3):720-5.
942 108. Kase H, Iwahashi K, Nakanishi S, Matsuda Y, Yamada K, Takahashi M, et al. K-252 compounds,
943 novel and potent inhibitors of protein kinase C and cyclic nucleotide-dependent protein kinases. Biochem
944 Biophys Res Commun. 1987;142(2):436-40.
945 109. Thuret G, Chiquet C, Herrag S, Dumollard JM, Boudard D, Bednarz J, et al. Mechanisms of
946 staurosporine induced apoptosis in a human corneal endothelial cell line. Br J Ophthalmol.
947 2003;87(3):346-52.
948 110. Green TP, Fennell M, Whittaker R, Curwen J, Jacobs V, Allen J, et al. Preclinical anticancer activity
949 of the potent, oral Src inhibitor AZD0530. Molecular oncology. 2009;3(3):248-61.
950 111. Rubenstein R, Sharma DR, Chang B, Oumata N, Cam M, Vaucelle L, et al. Novel Mouse Tauopathy
951 Model for Repetitive Mild Traumatic Brain Injury: Evaluation of Long-Term Effects on Cognition and
952 Biomarker Levels After Therapeutic Inhibition of Tau Phosphorylation. Front Neurol. 2019;10:124.
953 112. Zhao Z, Wang L, Volk AG, Birch NW, Stoltz KL, Bartom ET, et al. Regulation of MLL/COMPASS
954 stability through its proteolytic cleavage by taspase1 as a possible approach for clinical therapy of
955 leukemia. Genes Dev. 2019;33(1-2):61-74.
956 113. Segura-Egea JJ, Jimenez-Rubio A, Rios-Santos JV, Velasco-Ortega E, Calvo-Gutierrez JR. In vitro
957 inhibitory effect of EGTA on macrophage adhesion: endodontic implications. Journal of endodontics.
958 2003;29(3):211-3.
959 114. Knaryan VH, Samantaray S, Park S, Azuma M, Inoue J, Banik NL. SNJ-1945, a calpain inhibitor,
960 protects SH-SY5Y cells against MPP(+) and rotenone. J Neurochem. 2014;130(2):280-90.

bioRxiv preprint doi: https://doi.org/10.1101/821389; this version posted October 28, 2019. The copyright holder for this preprint (which was not certified by peer review) is the author/funder, who has granted bioRxiv a license to display the preprint in perpetuity. It is made available under aCC-BY 4.0 International license.

961 115. Henzing AJ, Dodson H, Reid JM, Kaufmann SH, Baxter RL, Earnshaw WC. Synthesis of novel caspase
962 inhibitors for characterization of the active caspase proteome in vitro and in vivo. J Med Chem.
963 2006;49(26):7636-45.
964 116. Chopra P, Gupta S, Dastidar SG, Ray A. Development of cell death-based method for the selectivity
965 screening of caspase-1 inhibitors. Cytotechnology. 2009;60(1-3):77.

966

967

968

969

970

971

972

973

974

975

976

977

978

979

980

981

982

983

984

985

986

bioRxiv preprint doi: https://doi.org/10.1101/821389; this version posted October 28, 2019. The copyright holder for this preprint (which was not certified by peer review) is the author/funder, who has granted bioRxiv a license to display the preprint in perpetuity. It is made available under aCC-BY 4.0 International license.

Figures. legends

Figure 1. OA induced tau hyperphosphorylation and oligomerization at different time points in mouse neuroblastoma N2a cells.

(a). Immunoblots of N2a cells extracted protein (20 µg) using total and phospho-tau antibodies: DA9 (a.a. 102-140), CP13 (pSer202), and PHF-1 (pSer396/pSer404). αII-Spectrin antibody was used to assess neuronal apoptotic pathway activation through monitoring intact spectrin (240 kDa), SBDP150/145 (calpain activation), and SBDP120 (caspase-3 activation). Different tau species are pointed with colored arrows. Blue arrows present monomeric p-tau (48 kDa), and oligomeric p-tau (110 kDa, 170 kDa, and 240 kDa). Red arrows on PHF-1 points on two minor bands of oligomeric p-tau (220 kDa and 260 kDa). Black arrows show non-phospho tau band (46 kDa). SNJ-1945 (abbreviated as S; a calpain inhibitor, 100 µM) and Z-DCB (abbreviated as Z; a caspase-3 inhibitor, 60 µM) were added for all experimental conditions for 1h before the treatment with OA (100 nM) for 6h or 24h, to prevent apoptosis-mediated proteolysis of tau and αII-Spectrin. A reverse time course followed OA treatment, and all cells were collected at the same time and conditions. (b). Immunoblots quantification. All data are normalized to β-actin and are expressed as a percentage of control. Data are presented as ± SEM for n=3. Statistical analysis was performed with one-way ANOVA. For multiple comparisons, one-way ANOVA followed by the Bonferroni's post-hoc test was performed. *$p<0.05$, **$p<0.01$, ***$p<0.001$, ****$p<0.0001$ and ns: non-significant. Full-length blots are presented in (**Supplementary Figure 4**).

Figure 2. **Screening of protein kinase inhibitors on OA-induced Tau hyperphosphorylation and oligomerization in N2a cells**.

bioRxiv preprint doi: https://doi.org/10.1101/821389; this version posted October 28, 2019. The copyright holder for this preprint (which was not certified by peer review) is the author/funder, who has granted bioRxiv a license to display the preprint in perpetuity. It is made available under aCC-BY 4.0 International license.

(a). Immunoblots of N2a cells extracted protein (20 µg) using phospho-tau antibodies (CP13, PHF-1), total tau (DA9), and αII-Spectrin. αII-Spectrin was probed to assess neuronal cell injury monitored with SBDP145/150 and SBDP120. Kinase inhibitors effect on OA-induced tau bands (100 nM) was monitored by evaluating the levels of monomeric (48 kDa) and oligomeric p-tau immunoreactivity (110 kDa, 170 kDa, and 240 kDa; blue arrows), total tau, and non-phospho tau (46 kDa; black arrows). Phosphorylated tau break-down products are shown with PHF-1 immunoblot. For all experimental conditions, S (a calpain inhibitor) and Z (a caspase-3 inhibitor) were added for 1h to before the addition of OA for 24h followed by 6h incubation with the kinase inhibitors. The concentrations used for each protein kinase inhibitor are mentioned in materials and methods, cell treatment section. β-actin was probed as a loading control. All experimental conditions were collected and analyzed at the same time. (b). Immunoblots quantification. All data are normalized to β-actin and are expressed as a percentage of control. Data are presented as ± SEM for n=3. Statistical analysis was performed with one-way ANOVA. For multiple comparisons, one-way ANOVA followed by the Bonferroni's post-hoc test was performed. *p<0.05, **p<0.01, ***p<0.001, ****p<0.0001 and ns: non-significant. Full-length blots are presented in (**Supplementary Figure** 5).

Figure 3. **Dose-response of TBB on OA-induced tau hyperphosphorylation and oligomerization in N2a cells.**

N2a cells were pre-treated with OA for 24h followed by treatment with different concentrations of TBB for 6h, as indicated in the figure. (a) Immunoblots of cell extracted proteins using phospho-tau antibodies, including CP13 (pSer202), and total tau DA9 (a.a. 102-140). Blue arrows represent monomeric and oligomeric p-tau (48 kDa, 110 kDa, and 170 kDa). αII-Spectrin antibody used to monitor SBDPs with the increasing concentrations of TBB. The β-actin antibody was used as a

bioRxiv preprint doi: https://doi.org/10.1101/821389; this version posted October 28, 2019. The copyright holder for this preprint (which was not certified by peer review) is the author/funder, who has granted bioRxiv a license to display the preprint in perpetuity. It is made available under aCC-BY 4.0 International license.

loading control. All conditions included SNJ-1945 (calpain inhibitor) and Z-DCB (caspase inhibitor). (b) TBB dose-response treatment line chart. TBB concentration (in micromolar) is shown on the X-axis, and the inhibition percentage is presented on the Y-axis. The control sample values were designated as the standard response. The X-axis concentration values are logarithm-transformed to fit a straight line. The half maximal inhibitory concentration (IC50) was used to measure the effectiveness of TBB in inhibiting OA-induced tau hyperphosphorylation and oligomerization. GraphPad Prism was used to calculate the IC50 (for DA9 and CP13 antibodies) and are presented in the figure. The statistical analysis was performed with one-way ANOVA, followed by Bonferroni's post-hoc test. *$p<0.05$, **$p<0.01$, ***$p<0.001$. Data are presented as ± SEM for n=3. Full-length blots are presented in (**Supplementary Figure 6**).

Figure 4. Screening of protein kinase inhibitors on physiologically phosphorylated tau in rat primary cerebrocortical neuronal culture.

Rat primary cerebrocortical neuronal differentiated cultures (CTX) at 15 DIVs, were treated various protein kinases inhibitors, including K252a (30 μM), STS (20 μM), LiCl (10 μM), EGTA (5 mM), Roscovitine (60 μM), Saracatinib (100 μM), TBB (30 μM) and A-107 (20 μM), AR (60 μM) for 6h. Calpain and caspase inhibitors (S+Z) were added to all experimental conditions for 1h before the protein kinase inhibitor treatments. Cell lysates were analyzed on western blots using twenty micrograms of protein. (a) Immunoblots of cell lysates analyzed for phosphorylated tau at the epitopes CP13 (pSer202), PHF-1 (pSer396/404), AT8 (pSer202/pThr205), RZ3 (pThr231), and AT270 (pThr181). Total tau was probed with DA31 (a.a. 150-190) antibody. DA31 blot showed two distinctive tau bands (63 kDa, non-phospho tau and 67 kDa, p-tau) following kinase inhibitors treatment. SBDP145/150 and SBDP120 were analyzed with the αII-spectrin antibody. Different lanes are numbered at the top of each label in the figure. (b) Immunoblot quantification

bioRxiv preprint doi: https://doi.org/10.1101/821389; this version posted October 28, 2019. The copyright holder for this preprint (which was not certified by peer review) is the author/funder, who has granted bioRxiv a license to display the preprint in perpetuity. It is made available under aCC-BY 4.0 International license.

of basal tau phosphorylation. Ratios of phospho-epitope levels over β-actin ± SD are represented as a percentage. Statistical analysis was performed with one-way ANOVA. For multiple comparisons, one-way ANOVA followed by the Bonferroni's post-hoc test was performed. *p<0.05, **p<0.01, ***p<0.001 and ****p<0.0001. n=3 per condition. Full-length blots are presented in (**Supplementary Figure 7**).

Figure 5. Effect of protein kinase inhibitors on OA-induced tau hyperphosphorylation in rat primary cerebrocortical neuronal culture.

Rat primary cerebrocortical neuronal differentiated cultures (CTX) at 15 DIV were treated with OA (100 nM) for 24h followed by protein kinases inhibitors for 6h. The concentrations of kinase inhibitors are the same as the ones mentioned in **Figure 4**. CTX cultures were treated with S and Z for 1h before any treatment to prevent apoptotic pathway-mediated tau proteolysis. (a). Immunoblots of cell lysates analyzed for phosphorylated tau at the epitopes CP13, PHF-1, AT8, RZ3, AT270. Total tau was probed with DA31 antibody. With DA31 blot, the 63 kDa band is referred to as monomeric non-phospho tau and the 67 kDa as monomeric p-tau species. Spectrin Break down products (SBDPs) were monitored with the αII-spectrin antibody. (b) Immunoblot quantification of OA-induced tau phosphorylation. Ratios of phospho-epitope levels over β-actin ± SD are represented as a percentage. Statistical analysis was performed with one-way ANOVA. For multiple comparisons, one-way ANOVA followed by the Bonferroni's post hoc test was performed. *p<0.05, **p<0.01, ***p<0.001 and ****p<0.0001. n=3 per condition. Full-length blots are presented in (**Supplementary Figure 8**).

Figure 6. The tauopathy-model and a proposed mechanism for various protein kinase inhibitors intervention.

bioRxiv preprint doi: https://doi.org/10.1101/821389; this version posted October 28, 2019. The copyright holder for this preprint (which was not certified by peer review) is the author/funder, who has granted bioRxiv a license to display the preprint in perpetuity. It is made available under aCC-BY 4.0 International license.

Dephosphorylated tau protein binds the microtubules to maintain it in the polymerized state. Phosphorylation of tau protein by a host of different kinases causes tau to dissociate from the microtubules. Dissociation of tau causes the microtubules to depolymerize. Specific phosphatases dephosphorylate tau allowing the microtubule to re-polymerize again, a physiological process that provides structure and shape to the cytoskeleton of neurons. In tauopathies, imbalances between kinases and phosphatases functions lead to tau hyperphosphorylation at particular pathological sites and a higher tendency to dissociate from the microtubules producing soluble tau aggregates and insoluble paired helical filaments (PHF), that could combine to form neurofibrillary tangles (NFT). NFT is known to be the toxic species in AD and CTE, including other tauopathy diseases and little is known about their active mechanism of neurodegeneration. OA inhibits the function of crucial tau phosphatases, (PP1 and PP2A) leading to activation of tau kinases and tau hyperphosphorylation initiating the pathological processes of tauopathies. One pharmaceutical approach to reverse the mechanism of tauopathies is kinase inhibition. The protein kinase inhibitors selected in this study are indicated on this figure. The inhibitors highlighted in blue are ones that showed a promising effect on our OA-induced cell-based tauopathy model. Microsoft PowerPoint was used to create the artwork.

Supplementary Figure 1: Effect of cyclosporin A on OA-induced tau hyperphosphorylation in mouse N2a cells.

The same experimental design mentioned in **Figure 2** was used to test CsA in N2a cell culture. Twenty micrograms of protein extract were used for the analysis of tau. Calpain and caspase-3 inhibitors (S+Z) were added to all experimental conditions, including the control samples. CsA is known to inhibit the phosphatase activity of calcineurin (PP3). In the presented experiment, it is used to assess its kinase inhibition potential on the monomeric and oligomeric p-tau induced by

bioRxiv preprint doi: https://doi.org/10.1101/821389; this version posted October 28, 2019. The copyright holder for this preprint (which was not certified by peer review) is the author/funder, who has granted bioRxiv a license to display the preprint in perpetuity. It is made available under aCC-BY 4.0 International license.

OA. (a). Immunoblots of N2a neuronal culture protein extracts showing antibodies directed against major tau phosphorylation sites. Two additional p-tau antibodies were used (AT270 and RZ3) to assess the phosphorylation sites at pThr181 and pThr231, respectively. RZ3 and AT270 detected distinctive monomeric p-tau bands at 48 kDa, and 55 kDa, respectively. Total tau levels were probed using DA9 (a.a. 102-145) in N2a cells. Blue colored labels correspond to monomeric or oligomeric p-tau species. Immunoblots were probed with αII-spectrin antibody to monitor calpain and caspase-3 mediated proteolysis. (b). Immunoblots quantification of N2a. The ratio of phosphorylation epitopes levels over β-actin levels ± SD are represented as a percentage of control. n=3 per condition. For multiple comparisons, one-way ANOVA followed by the Bonferroni's post-hoc test was performed. *p<0.05, **p<0.01, ***p<0.001, ****p<0.0001, ns: non-significant.

Supplementary Figure 2. Effect of additional two GSK-3 protein kinase inhibitors on OA-induced tau hyperphosphorylation and oligomerization in N2a cells (with cell-death linked protease inhibitors (calpain/caspase inhibitors).

A continuation of Figure 2 experiment is presented to include two other potent GSK-3 kinase inhibitors, AR and A-107. The detailed experimental treatments are as described in materials and methods. (a). Immunoblots of N2a cells extracted protein using p-tau antibodies (CP13 and PHF-1), total tau (DA9), and αII-Spectrin. αII-Spectrin was probed to assess cell apoptosis monitored SBDP150/145 kDa and SBDP120 kDa. Kinase inhibition of phosphorylation and oligomerization was monitored by evaluating the levels of p-tau antibodies and total tau (blue arrows) and non-phospho tau (black arrows). For all conditions, S+Z were added for 1h before the treatments. (b). Immunoblots quantification and statistical analysis. All data are normalized to β-actin and are expressed as a percentage of control. Data are presented as ± SEM for n=3. Statistical analysis was

bioRxiv preprint doi: https://doi.org/10.1101/821389; this version posted October 28, 2019. The copyright holder for this preprint (which was not certified by peer review) is the author/funder, who has granted bioRxiv a license to display the preprint in perpetuity. It is made available under aCC-BY 4.0 International license.

performed with one-way ANOVA. For multiple comparisons, one-way ANOVA followed by the Bonferroni's post-hoc test was performed. *p<0.05, **p<0.01, ***p<0.001, ****p<0.0001 and ns: non-significant.

Supplementary Figure 3. Cyclosporin A inhibits physiological and OA-induced Tau hyperphosphorylation in rat primary cerebrocortical neuronal culture.

The experimental procedures were followed as described in **Figure 4** and **Figure 5** legends. Primary neuronal cultures (CTX) were fully differentiated and had healthy neurites when examined under the microscope. All wells were pretreated with S+Z for 1h. For conditions that did not include OA, cultures were treated with CsA for 6h. For OA-induced conditions, OA was added for 24h followed by CsA for 6h. A reverse time course was followed, and all experimental conditions were collected and analyzed at the same time. Twenty micrograms of CTX culture extracts were run on SDS-PAGE followed by western blotting. (a). Immunoblots of CTX culture protein extracts. CTX culture using antibodies directed against major tau phosphorylation sites including: CP13 (pSer202), PHF-1 (pSer396/pSer404), RZ3 (pThr231), AT8 (pSer202/pThr205), AT270 (pThr181). Total tau levels were probed using DA31 (a.a. 102-145). The 67 kDa assigned as monomeric p-tau band and the 63 kDa band was assigned as monomeric non-phospho tau at the different studied epitopes. (b). Immunoblots quantification. The ratio of phosphorylation epitopes levels over β-actin levels ± SD are represented as a percentage of control. n=3 per condition. For multiple comparisons, one-way ANOVA followed by the Bonferroni's post-hoc test was performed. *p<0.05, **p<0.01, ***p<0.001, ****p<0.0001, ns: non-significant.

Supplementary Figure 4. Full scanned immunoblots for Figure 1a.

Supplementary Figure 5. Full scanned immunoblots for Figure 2a.

Supplementary Figure 6. Full scanned immunoblots for Figure 3a.

bioRxiv preprint doi: https://doi.org/10.1101/821389; this version posted October 28, 2019. The copyright holder for this preprint (which was not certified by peer review) is the author/funder, who has granted bioRxiv a license to display the preprint in perpetuity. It is made available under aCC-BY 4.0 International license.

Supplementary Figure 7. Full scanned immunoblots for Figure 4a.

Supplementary Figure 8. Full scanned immunoblots for Figure 5a.

Table 1. Phosphatase, Kinase inhibitor and other pharmacological agents used in the study.

Table 2. Antibodies used in this study.

Table 3. Composite effects of kinase inhibitors on OA-induced Tau hyperphosphorylation in N2a cells.

Table 4. Composite effects of kinase inhibitors on basal and OA-induced Tau hyperphosphorylation in rat primary cerebrocortical neuronal cells.

bioRxiv preprint doi: https://doi.org/10.1101/821389; this version posted October 28, 2019. The copyright holder for this preprint (which was not certified by peer review) is the author/funder, who has granted bioRxiv a license to display the preprint in perpetuity. It is made available under aCC-BY 4.0 International license.

Table 1. Phosphatase, Kinase inhibitor and other pharmacological agents used in the study

Agent	Full Name / Function	Target	Affinity in vitro (Ki)	Cross- reactivities	IC_{50} (cell-based assay)
Phosphatase Inhibitors					
OA	Okadaic Acid, Serine/Threonine phosphatase activity	PP1, PP2A inhibitor	150 nM, 32 pM (102)	----------	0.1 µM(103)
CsA	Cyclosporin A/calcium dependent protein phosphatase - immunosuppressant	Calcineurin (PP3)	0.98 µM(104)	FK-506	55 µM(105)
Kinase Inhibitors					
LiCl	Lithium Chloride – acts by competing for magnesium.	GSK3β	1-2 mM(106)	----------	1-2 mM(107)
AR-A014418	N-(4-methoxybenzyl)-N'-(5-nitro-1,3-thiazol-2-yl) urea, antidepressant. Inhibits in an ATP competitive manner	GSK3β	38 nM(91)	----------	104±27 nM (91)
A-1070722	1-(7-methoxyquinolin-4-yl)-3-(6-(trifluoromethyl) pyridin-2-yl) urea Brain penetrant. Inhibits in an ATP competitive manner.	GSK-3α and GSK-3β	0.6 nM(59)	----------	35-66 nM(90)
K252a	Staurosporine analog, non-selective cell permeable Protein Kinase Inhibitor	PKA, PKC, PKG, CaMK, and phosphorylase kinase, and others	1.8-20 nM(108)	Broad kinase inhibitor	1.3-3 µM(63)
STS	Staurosporine, highly non-selective cell permeable Protein Kinase Inhibitor	Pan Protein Kinase Inhibitor	3-15 nM	Broad kinase inhibitor	0.5 µM(109)
AZD0530	Saracatinib, anti-invasive and anti-tumor activities	Src/Fyn Tyrosine Kinase inhibitor	5-10 nM(21)	Brc-Abl tyrosine kinase	1- 10 µM(110)
Roscovitine	Seliciclib, competes for the ATP binding sites, apoptotic and antineoplastic activity	CDK5/P35 inhibitor	0.2 µM(66)	Pyridoxal Kinase (non-protein target)	10 µM (111)
TBB	4,5,6,7-tetrabromobenzotriazole, Acts in an ATP/GTP-competitive manner by binding to the Val66 residue of casein kinase-2.	CKII inhibitor	80-210 nM(112)	----------	10 µM (from the present study)
Calcium Chelators					
EGTA	ethylene glycol-bis (β-aminoethyl ether)-N, N, N', N'-tetraacetic acid, chelator of divalent cations.	divalent ion chelator (Ca^{2+} /Mg^{2+})	10 nM(113)	Tyr kinase (500 nM)	2-5 mM(113)
Other Inhibitors					
SNJ-1945	Amphipathic ketoamide – neuroprotective cell-permeable calpain inhibitor	Calpain 1, 2 inhibitors	100 nM(114)	----------	20-30 µM(114)
Z-DCB	Z-Asp-2,6-Dichlorobenzoyloxymethyl Ketone, Inactivates the interleukin-1β-converting enzyme	Pan-Caspase inhibitor	1-10 µM(115)	Inhibit the production of cytokines in human peripheral blood mononuclear cells and T cell proliferation	20-50 µM(116)

1169

1170

bioRxiv preprint doi: https://doi.org/10.1101/821389; this version posted October 28, 2019. The copyright holder for this preprint (which was not certified by peer review) is the author/funder, who has granted bioRxiv a license to display the preprint in perpetuity. It is made available under aCC-BY 4.0 International license.

Table 2. Antibodies used in this study

Clone name	Epitope*	Supplier (Catalog#)	MAb/ PAb
Phospho Tau antibodies			
AT8	pSer202/pThr205	Fisher-Thermo (MN1020)	Mouse MAb
AT270	pThr181	Fisher-Thermo (MN1050)	Mouse MAb
RZ3	pThr231	Peter Davies, Albert Einstein College of Medicine, Bronx, NY	Mouse Mab
CP13	pSer202	Peter Davies, Albert Einstein College of Medicine, Bronx, NY	Mouse MAb
PHF-1	pSer396/pSer404	Peter Davies, Albert Einstein College of Medicine, Bronx, NY	Mouse Mab
Total Tau Antibodies			
DA9	aa102-140	Peter Davies, Albert Einstein College of Medicine, Bronx, NY	Mouse Mab
DA31	aa150–190	Peter Davies, Albert Einstein College of Medicine, Bronx, NY	Mouse Mab

*Epitope based on human Tau-441 sequence.

bioRxiv preprint doi: https://doi.org/10.1101/821389; this version posted October 28, 2019. The copyright holder for this preprint (which was not certified by peer review) is the author/funder, who has granted bioRxiv a license to display the preprint in perpetuity. It is made available under aCC-BY 4.0 International license.

Table 3. Composite effects of kinase inhibitors on OA-induced Tau hyperphosphorylation in N2a cells.

Inhibitor	Inhibition %		
	CP13 (110 kDa)	PHF-1 (240 kDa)	DA9 (170 kDa)
K252a	62	70	40
STS	32	82	-10
LiCl	-14	-9	-12
EGTA	90	85	55
CsA	98	90	**100**
Roscovitine	-11	-53	-22
TBB	**100**	**100**	**100**
Saracatinib	70.5	46	45
A107	23	0	13
AR	0	0	36

A negative sign correspond to an adverse effect. Bold corresponds to maximal inhibition at the tested epitope.

bioRxiv preprint doi: https://doi.org/10.1101/821389; this version posted October 28, 2019. The copyright holder for this preprint (which was not certified by peer review) is the author/funder, who has granted bioRxiv a license to display the preprint in perpetuity. It is made available under aCC-BY 4.0 International license.

Table 4. Composite effects of kinase inhibitors on basal and OA-induced Tau hyperphosphorylation in rat primary cerebrocortical neuronal cells.

Inhibitor		Inhibition %					
		CP13	**RZ3**	**PHF-1**	**AT8**	**AT270**	**DA31**
K252a	- OA	35	45	61	10	17	41
	+ OA	41	37	63	0	0	45
STS	- OA	86	83	55	88	**100**	79
	+ OA	63	81	89	12	**100**	77
LiCl	- OA	94	89	98	**100**	**100**	93
	+ OA	50	100	100	81	**100**	96
EGTA	- OA	-51	-63	-22	-64	-68	-73
	+ OA	-12	-22	-13	-5	-63	-69
Roscovitine	- OA	85	42	63	91	**100**	32
	+ OA	63	91	81	0	18	29
TBB	- OA	91	**100**	**100**	91	**100**	41
	+ OA	98	**100**	**100**	**100**	**100**	91
Saracatinib	- OA	41	81	52	0	0	5
	+ OA	**100**	**100**	**100**	0	84	20
A-107	- OA	92	79	65	82	**100**	80
	+ OA	36	70	85	21	**100**	55
AR	- OA	**100**	89	**100**	**100**	**100**	**100**
	+ OA	89	**100**	**100**	**100**	**100**	**100**
CsA	- OA	90	91	89	95	92	95
	+ OA	33	26	0	86	11	28

A negative sign correspond to an adverse effect. Bold corresponds to maximal inhibition at the tested epitope. The -/+ OA indicates either the presence or absence of okadaic acid compound. The densitometric intensity of 67 kDa band from **Figure 4** and **Figure 5** was used for calculating the percentage of inhibition.

Figure 1

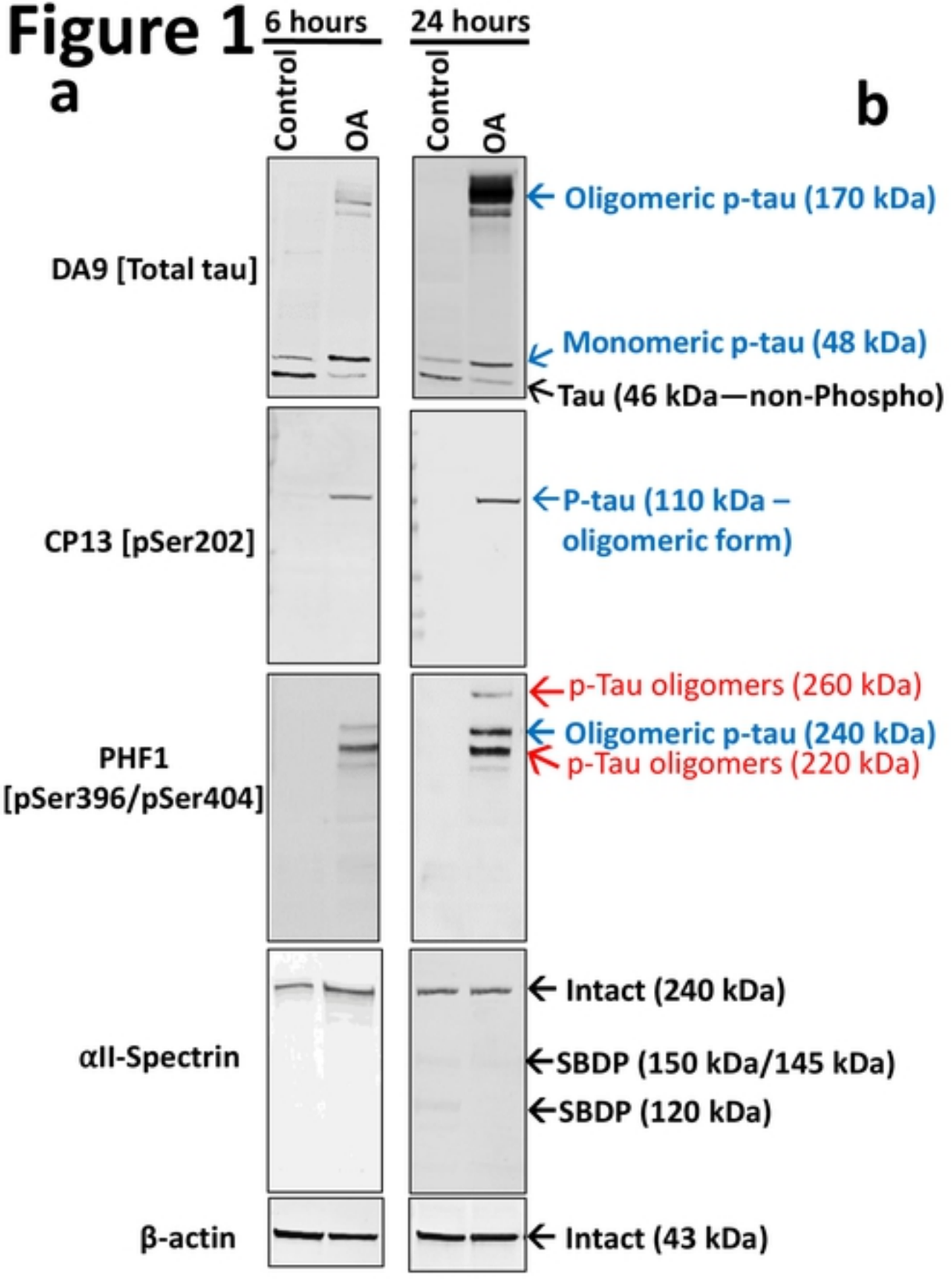
a
6 hours
24 hours
Control
OA
Control
OA
DA9 [Total tau]
CP13 [pSer202]
PHF1
[pSer396/pSer404]
αII-Spectrin
β-actin
Oligomeric p-tau (170 kDa)
Monomeric p-tau (48 kDa)
Tau (46 kDa—non-Phospho)
P-tau (110 kDa –
oligomeric form)
p-Tau oligomers (260 kDa)
Oligomeric p-tau (240 kDa)
p-Tau oligomers (220 kDa)
Intact (240 kDa)
SBDP (150 kDa/145 kDa)
SBDP (120 kDa)
Intact (43 kDa)

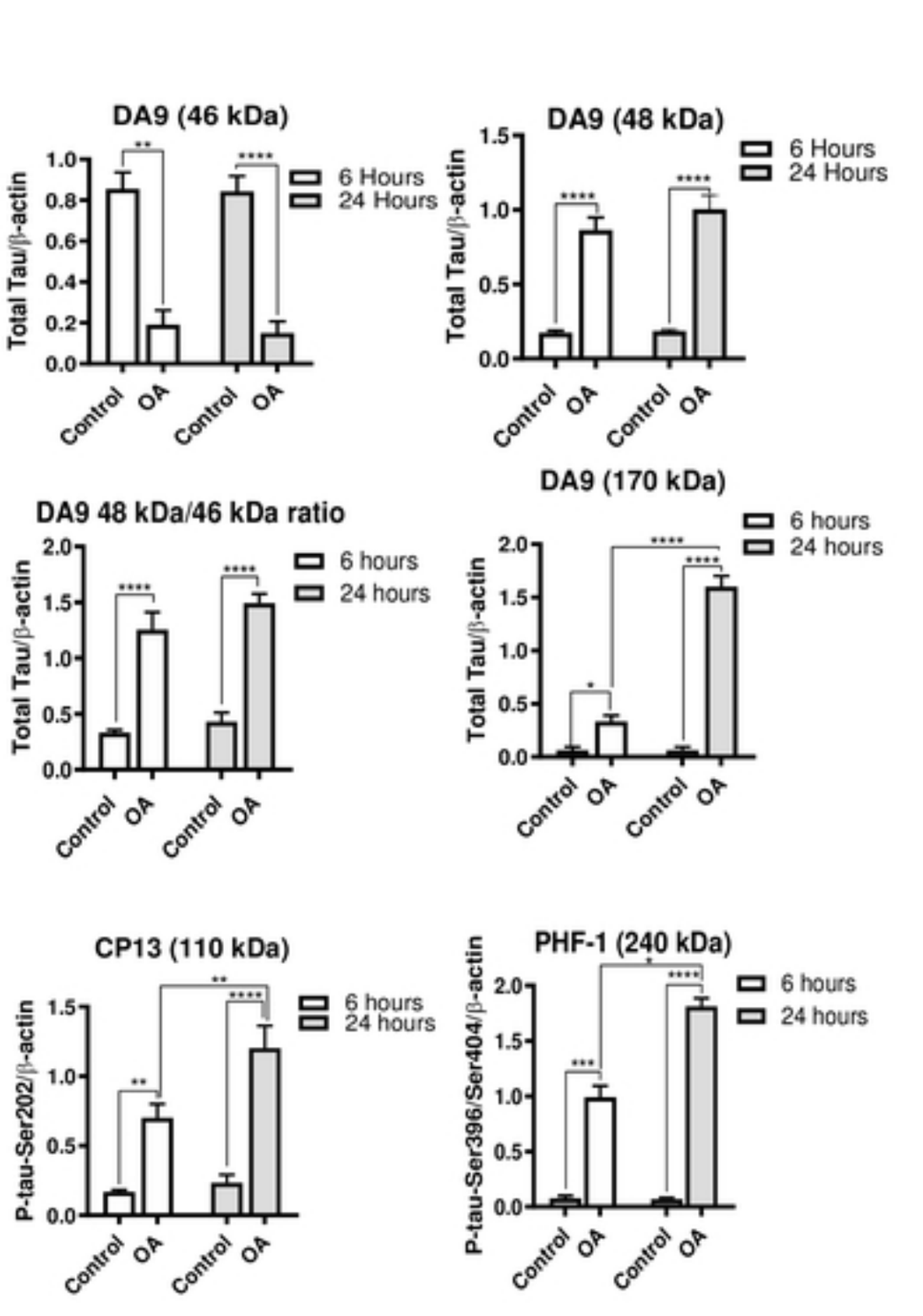
b
DA9 (46 kDa)
Total Tau/β-actin
6 Hours
24 Hours
Control
OA
DA9 (48 kDa)
DA9 48 kDa/46 kDa ratio
6 hours
24 hours
DA9 (170 kDa)
CP13 (110 kDa)
P-tau-Ser202/β-actin
PHF-1 (240 kDa)
P-tau-Ser396/Ser404/β-actin

Figure 2

a

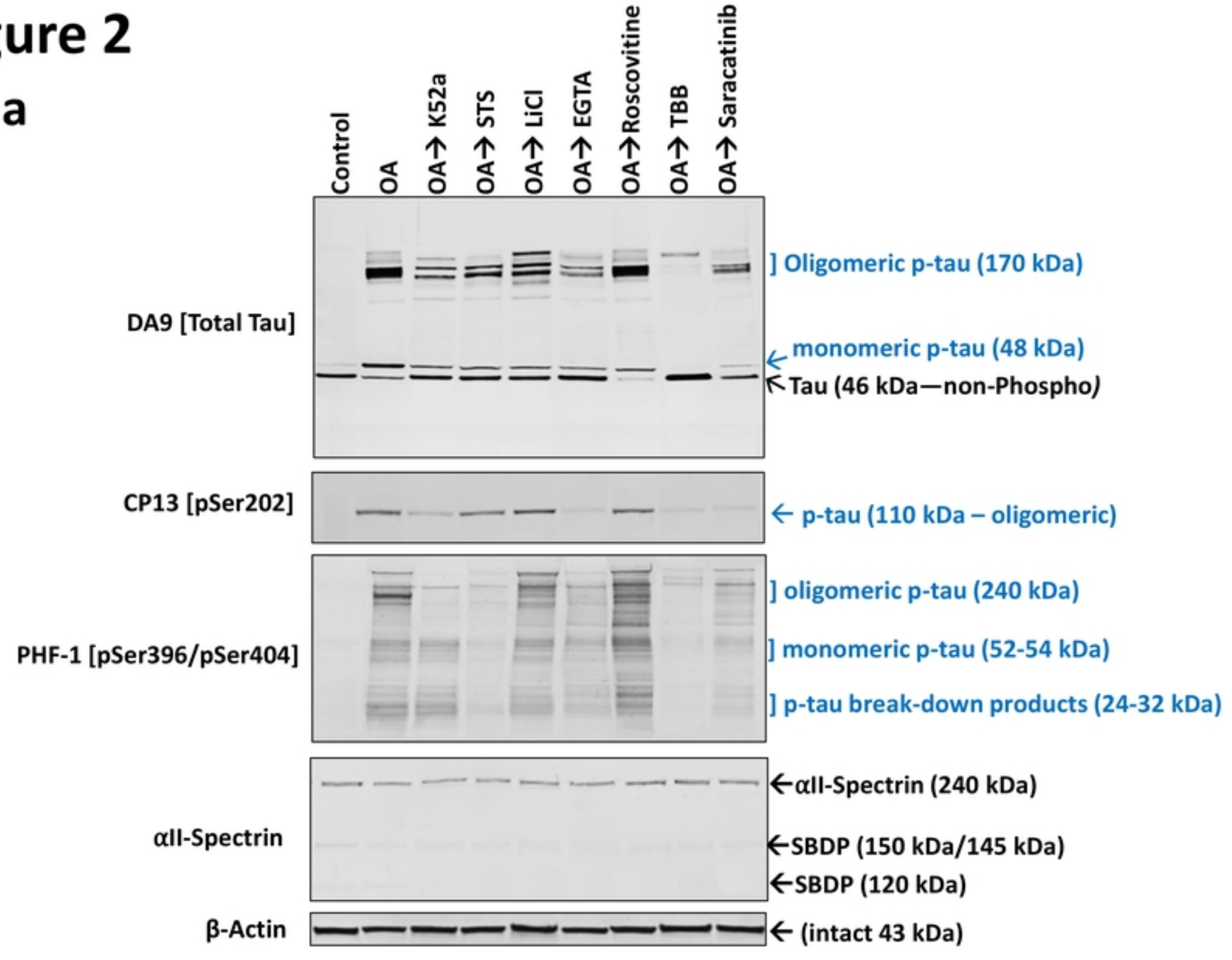
Control
OA
OA→ K52a
OA→ STS
OA→ LiCl
OA→ EGTA
OA→Roscovitine
OA→ TBB
OA→ Saracatinib
DA9 [Total Tau]
] Oligomeric p-tau (170 kDa)
monomeric p-tau (48 kDa)
Tau (46 kDa—non-Phospho)
CP13 [pSer202]
← p-tau (110 kDa – oligomeric)
PHF-1 [pSer396/pSer404]
] oligomeric p-tau (240 kDa)
] monomeric p-tau (52-54 kDa)
] p-tau break-down products (24-32 kDa)
αII-Spectrin
←αII-Spectrin (240 kDa)
←SBDP (150 kDa/145 kDa)
←SBDP (120 kDa)
β-Actin
← (intact 43 kDa)

1.

Figure 2

b

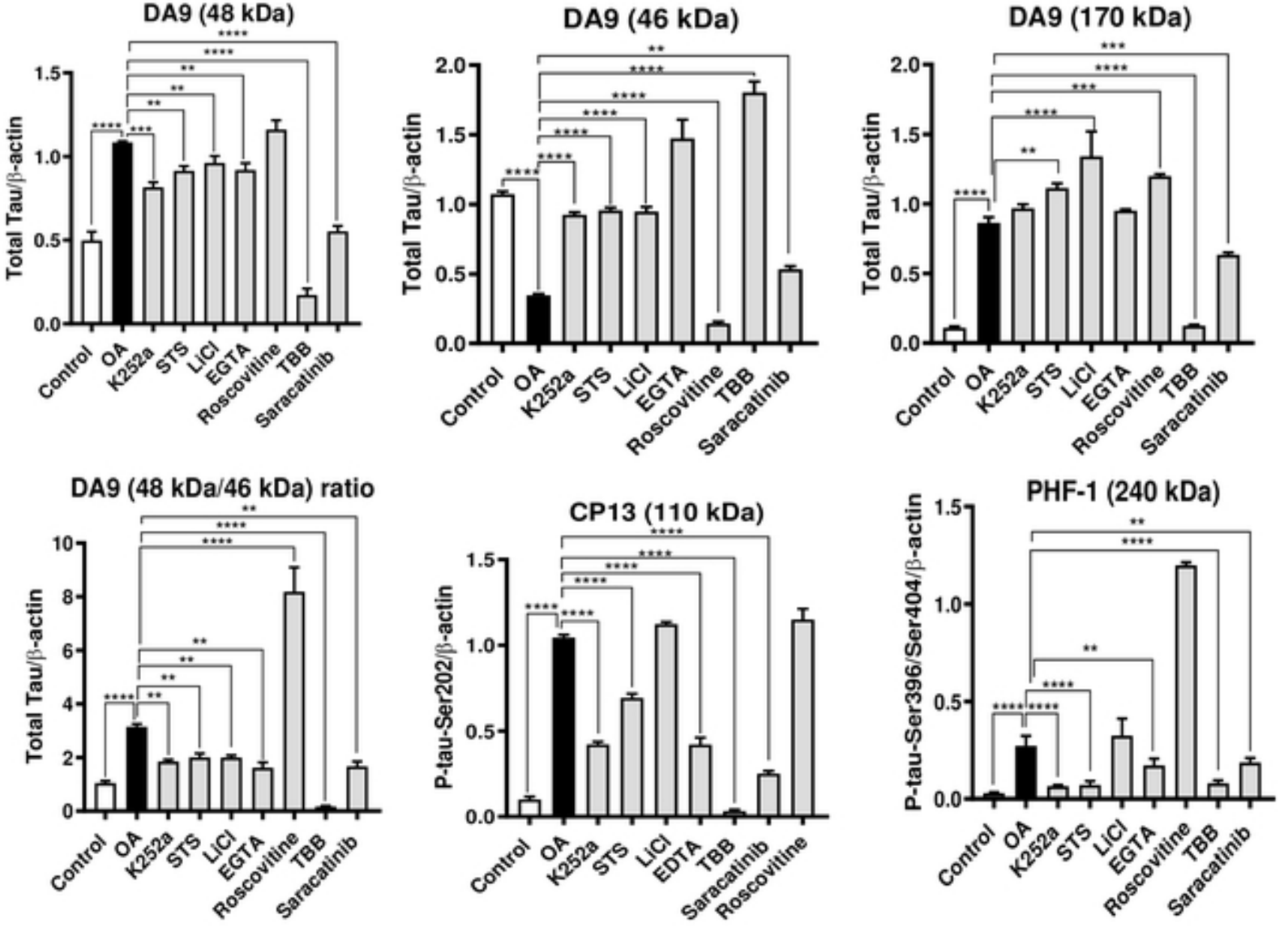
DA9 (48 kDa)
Total Tau/β-actin
Control
OA
K252a
STS
LiCl
EGTA
Roscovitine
TBB
Saracatinib
DA9 (46 kDa)
DA9 (170 kDa)
DA9 (48 kDa/46 kDa) ratio
CP13 (110 kDa)
P-tau-Ser202/β-actin
EDTA
PHF-1 (240 kDa)
P-tau-Ser396/Ser404/β-actin

Figure 3

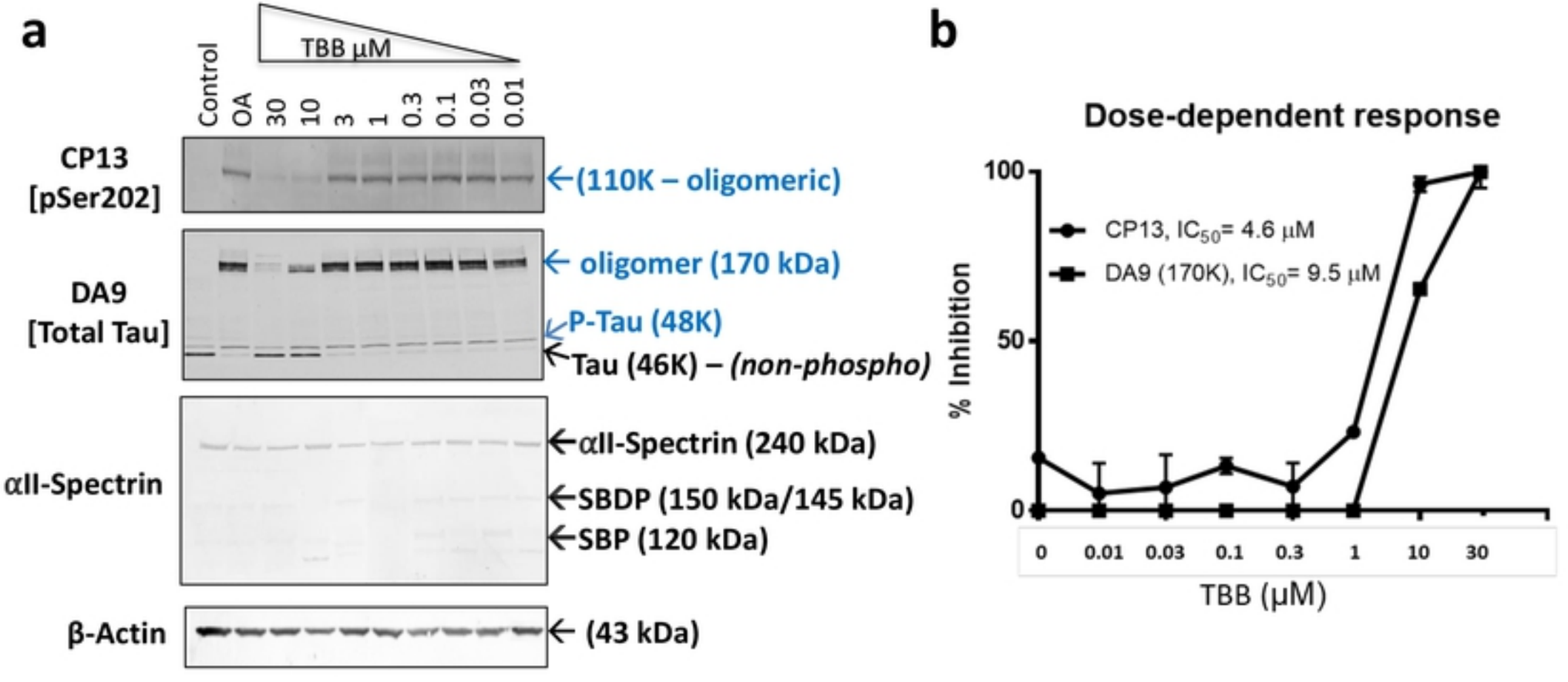
a
TBB µM
Control
OA
30
10
3
1
0.3
0.1
0.03
0.01
CP13
[pSer202]
←(110K – oligomeric)
DA9
[Total Tau]
← oligomer (170 kDa)
P-Tau (48K)
Tau (46K) – (non-phospho)
αII-Spectrin
αII-Spectrin (240 kDa)
SBDP (150 kDa/145 kDa)
SBP (120 kDa)
β-Actin
← (43 kDa)
b
Dose-dependent response
CP13, IC50= 4.6 µM
DA9 (170K), IC50= 9.5 µM
% Inhibition
100
50
0
0
0.01
0.03
0.1
0.3
1
10
30
TBB (µM)

Figure 4

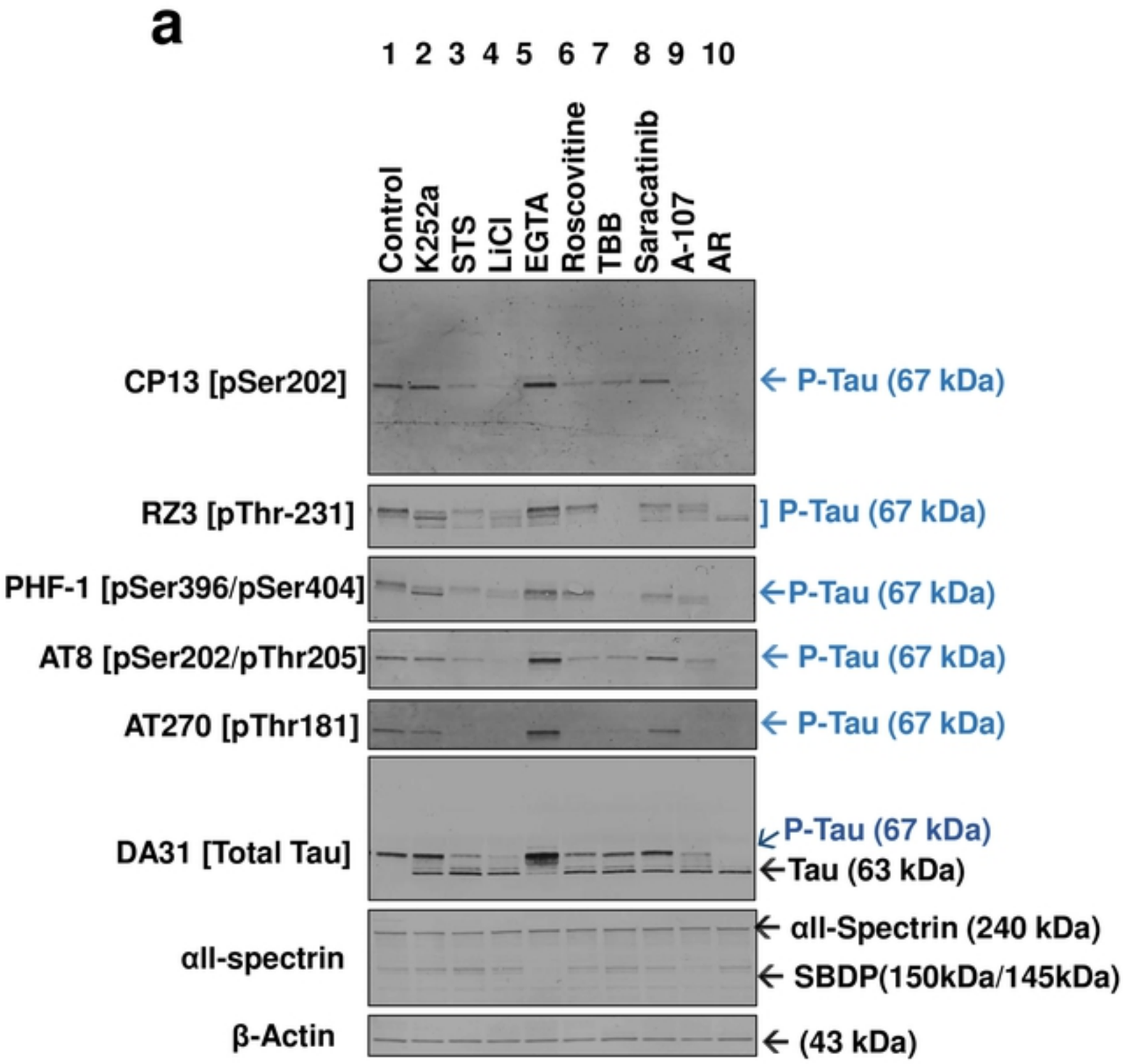
a
1 2 3 4 5 6 7 8 9 10
Control
K252a
STS
LiCl
EGTA
Roscovitine
TBB
Saracatinib
A-107
AR
CP13 [pSer202]
← P-Tau (67 kDa)
RZ3 [pThr-231]
] P-Tau (67 kDa)
PHF-1 [pSer396/pSer404]
←P-Tau (67 kDa)
AT8 [pSer202/pThr205]
← P-Tau (67 kDa)
AT270 [pThr181]
← P-Tau (67 kDa)
DA31 [Total Tau]
P-Tau (67 kDa)
←Tau (63 kDa)
αII-spectrin
← αII-Spectrin (240 kDa)
← SBDP(150kDa/145kDa)
β-Actin
← (43 kDa)

Figure 4

b

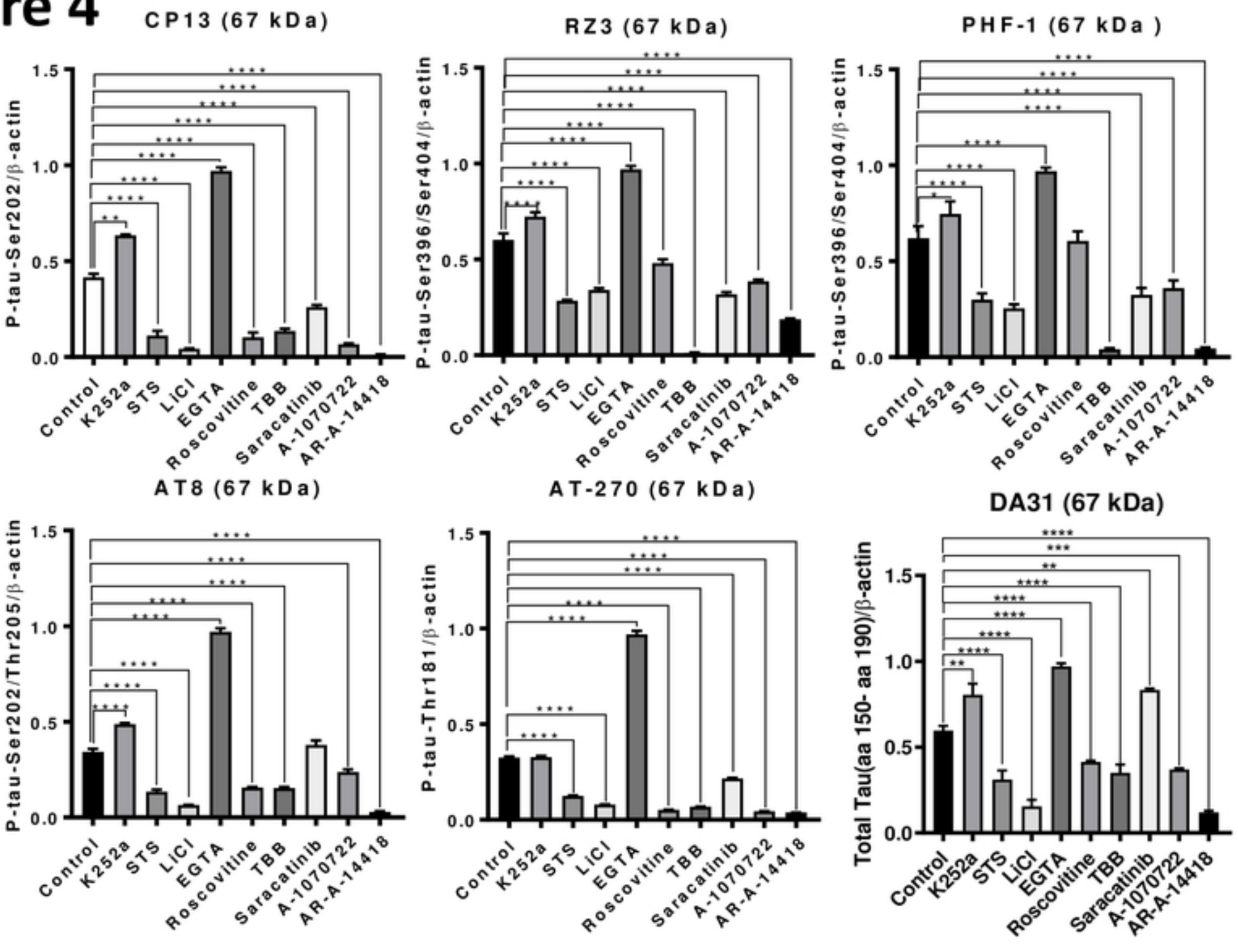
CP13 (67 kDa)
RZ3 (67 kDa)
PHF-1 (67 kDa)
AT8 (67 kDa)
AT-270 (67 kDa)
DA31 (67 kDa)
P-tau-Ser202/β-actin
P-tau-Ser396/Ser404/β-actin
P-tau-Ser202/Thr205/β-actin
P-tau-Thr181/β-actin
Total Tau(aa 150- aa 190)/β-actin
Control
K252a
STS
LiCl
EGTA
Roscovitine
TBB
Saracatinib
A-1070722
AR-A-14418

Figure 5

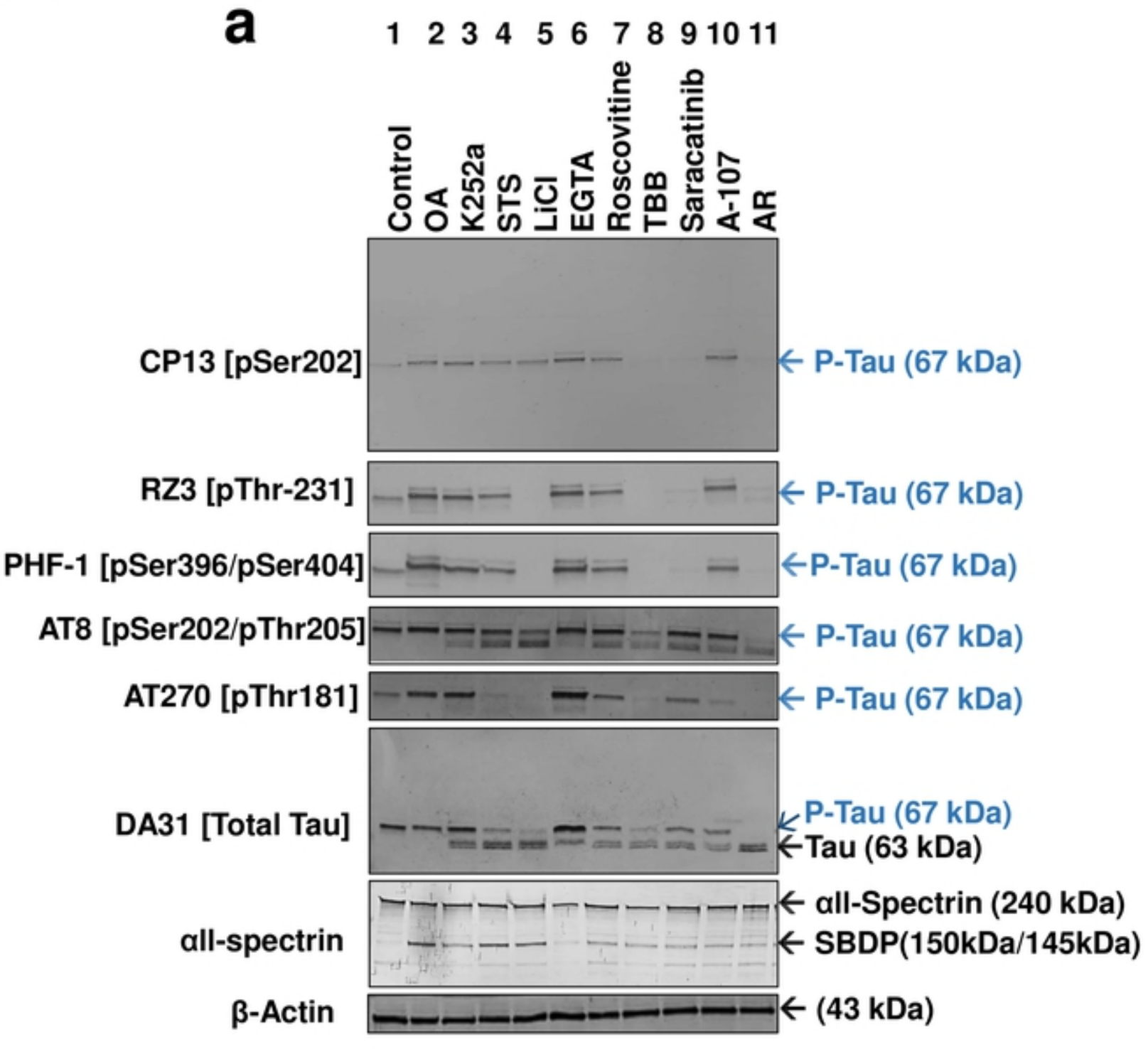
a
1 2 3 4 5 6 7 8 9 10 11
Control
OA
K252a
STS
LiCl
EGTA
Roscovitine
TBB
Saracatinib
A-107
AR
CP13 [pSer202]
← P-Tau (67 kDa)
RZ3 [pThr-231]
← P-Tau (67 kDa)
PHF-1 [pSer396/pSer404]
←P-Tau (67 kDa)
AT8 [pSer202/pThr205]
← P-Tau (67 kDa)
AT270 [pThr181]
← P-Tau (67 kDa)
DA31 [Total Tau]
P-Tau (67 kDa)
←Tau (63 kDa)
αII-spectrin
← αII-Spectrin (240 kDa)
← SBDP(150kDa/145kDa)
β-Actin
← (43 kDa)

Figure 5

b

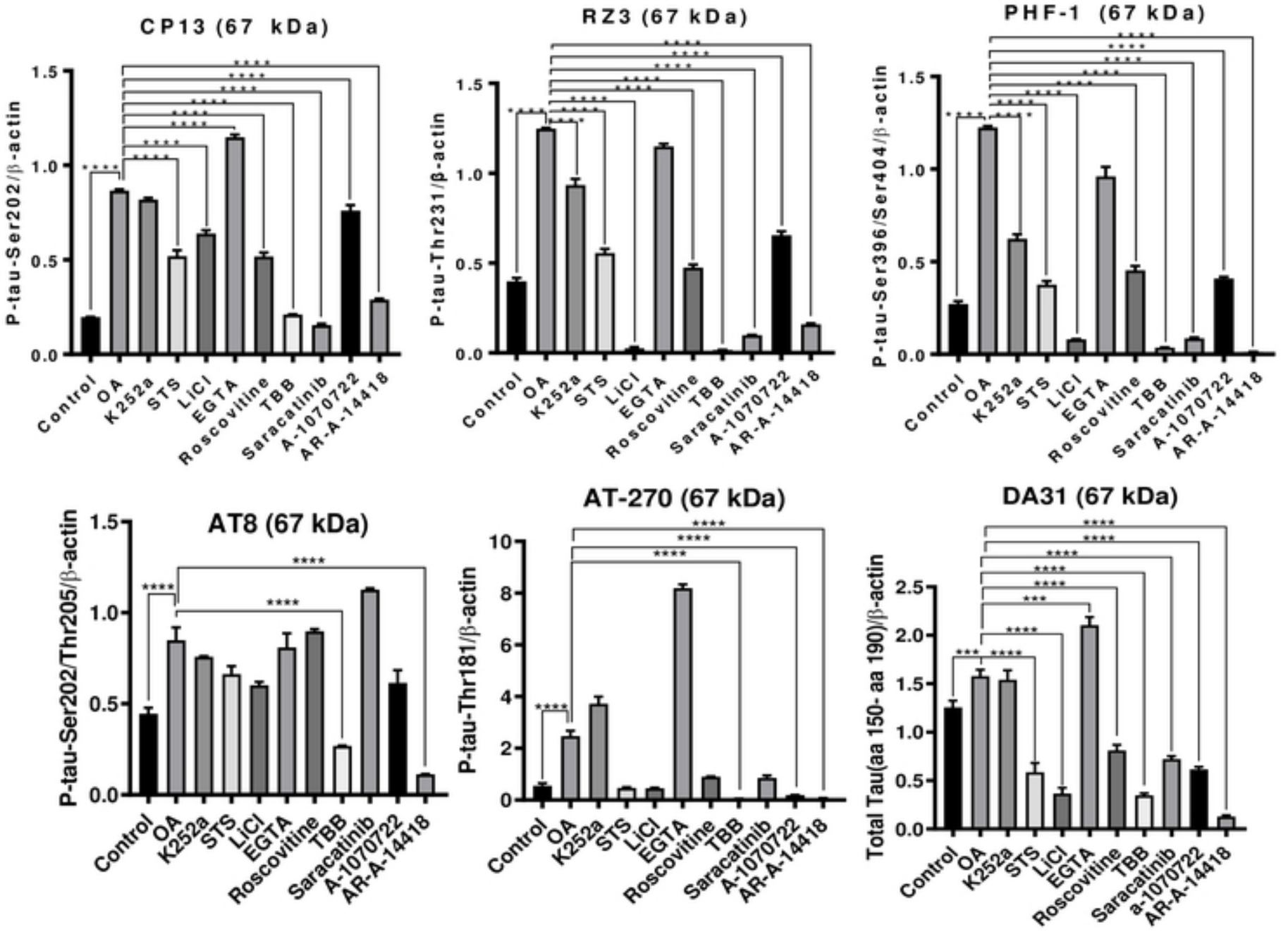
CP13 (67 kDa)
P-tau-Ser202/β-actin
RZ3 (67 kDa)
P-tau-Thr231/β-actin
PHF-1 (67 kDa)
P-tau-Ser396/Ser404/β-actin
AT8 (67 kDa)
P-tau-Ser202/Thr205/β-actin
AT-270 (67 kDa)
P-tau-Thr181/β-actin
DA31 (67 kDa)
Total Tau(aa 150- aa 190)/β-actin
Control
OA
K252a
STS
LiCl
EGTA
Roscovitine
TBB
Saracatinib
A-1070722
AR-A-14418
a-1070722

Figure 6

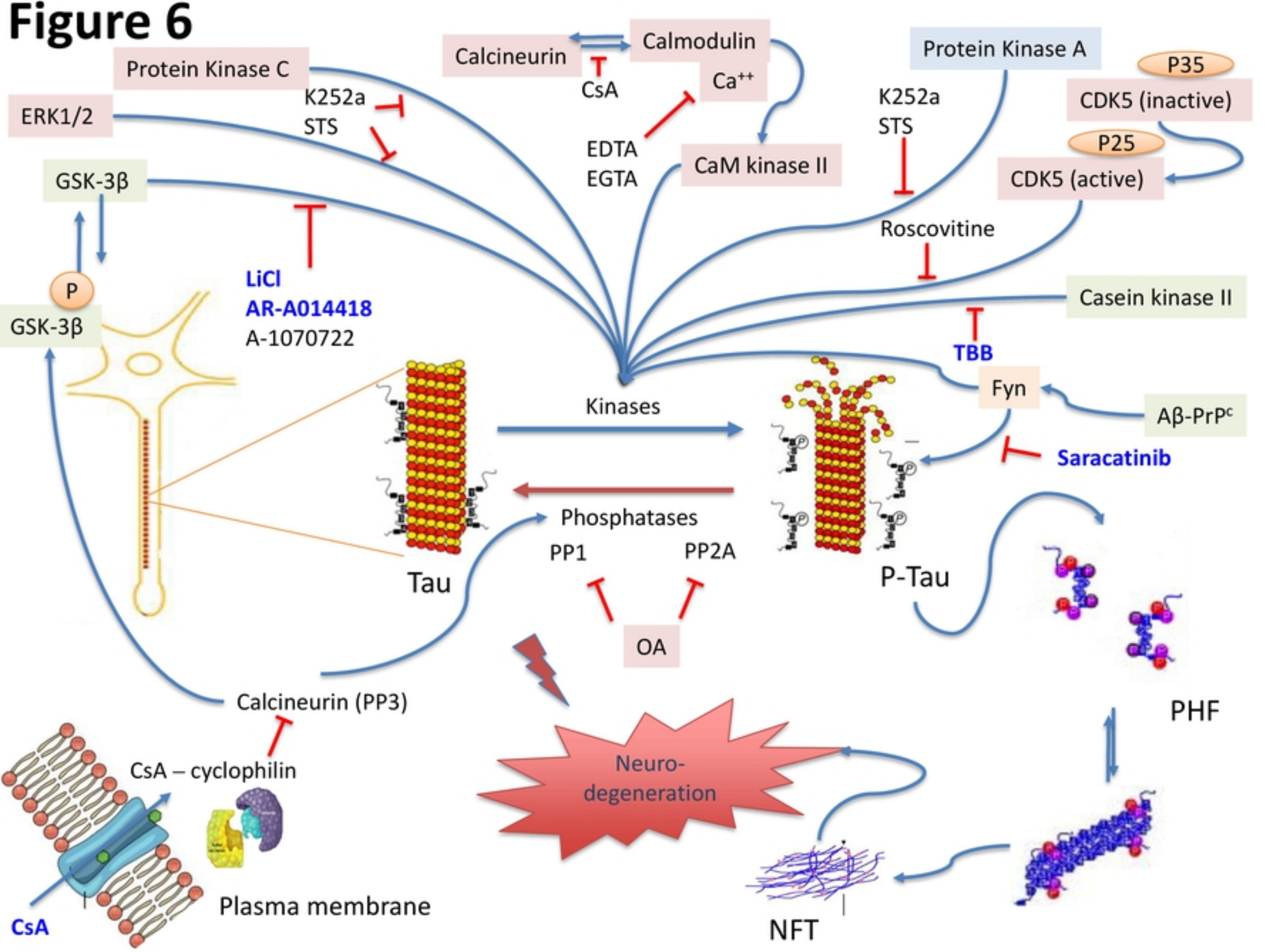
Protein Kinase C
ERK1/2
GSK-3β
P
GSK-3β
K252a
STS
LiCl
AR-A014418
A-1070722
Calcineurin
Calmodulin
CsA
Ca++
EDTA
EGTA
CaM kinase II
Protein Kinase A
K252a
STS
P35
CDK5 (inactive)
P25
CDK5 (active)
Roscovitine
Casein kinase II
TBB
Fyn
Aβ-PrPc
Saracatinib
Kinases
Phosphatases
PP1
PP2A
OA
Tau
P-Tau
PHF
NFT
Neuro-
degeneration
Calcineurin (PP3)
CsA – cyclophilin
Plasma membrane
CsA